ABSTRACT

Title of Document:	PARAMETRIC STUDY OF SOIL DRYING IN THE FIELD FOR COMPACTION QUALITY ASSURANCE
	Zahra Afsharikia, Master of Science, 2017
Directed By:	Professor Charles W. Schwartz, Department of Civil and Environmental Engineering

Moving towards modulus based methods of soil compaction quality assurance using lightweight deflectometers (LWD) requires evaluation of the LWD measured modulus in the field. The resilient modulus of geomaterials is not only influenced by the moisture content (MC) at the time of compaction, but also by the MC at the time of testing, which may be up to few hours after compaction. A parametric study was performed using SoilVision's SVFlux analysis package to model the variation of soil moisture profile with depth versus time as a function of environmental factors. Then the drying in a compacted soil layer was modeled and compared to the volumetric water content measurements in an instrumented large-scale test pit. Finally, LWD modulus values in the field were captured immediately and a few hours after compaction to exhibit the variation of modulus with time and to identify if the stiffness gain in geomaterial is significant.

PARAMETRIC STUDY OF SOIL DRYING IN THE FIELD FOR COMPACTION QUALITY ASSURANCE

By

Zahra Afsharikia

Thesis submitted to the Faculty of the Graduate School of the
University of Maryland, College Park, in partial fulfillment
of the requirements for the degree of
Master of Science
2017

Advisory Committee:
Professor Charles W. Schwartz, Chair
Professor M. Sherif Aggour
Professor Ahmet H. Aydilek

Dedication

To my parents, Sarah and Alireza, for their endless love and unfailing support.
To my little sister, Neshat, who is always there to make me smile.

Acknowledgements

Firstly, I would like to express my sincere gratitude to my advisor Professor Charles Schwartz for the continuous support of my study at University of Maryland, for his patience, motivation, and immense knowledge. His brilliant guidance helped me in all the time of research and writing of this thesis.

I am also grateful to my thesis committee, Professor M. Sherif Aggour, Professor Dimitrios Goulias, and Professor Ahmet Aydilek for their insightful comments and encouragement.

My sincere thanks to Dr. Murray Fredlund and SoilVision family for providing valuable support and enlightenment during software installation and modeling.

I am also thankful to the MD, FL, MO, and NY Departments of Transportations for their contribution to this research and all agencies participating the Transportation Pooled Fund study program—TPF 5(825) including VDOT, MDOT, NCDOT, and SCDOT. A very special gratitude goes to Dan Sajedi from Maryland State Highway Administration (MDSHA) for his devotion and leadership.

Appreciation to Dr. Nelson Gibson from the Federal Highway Administration (FHWA) to make it possible to perform testing at the Turner-Fairbank Highway Research (TFHRC). Thanks also to our LWD device providers, Virginia and Garry Aicken of Kessler Soils Engineering Inc. representative of Zorn Instruments, Larry Olson and Pat Miller of Olson Engineering, and Dr. Sadaf Khosravifar and Regis Carvalho of Dynatest Consulting Inc.

Finally, I thank my fellow lab mates Dr. Sadaf Khosravifar, Gregory Koepping, Ramiz Vatan, Marcus Lapa Watson, and Mateus Coelho for their stimulating discussions and assistance during the field and lab testing and to all my friends who supported me through the sleepless nights. You truly made the impossible possible.

Table of Contents

List of Tables

List of Figures

1. Chapter 1: Introduction

1.1. Motivation for the study

Compaction control for unbound material is traditionally based on maximum dry density and optimum moisture content as determined from the Proctor compaction tests (AASHTO T 99 or T 180) in the laboratory. Moving away from traditional methods of compaction quality assurance (QA), modulus-based approaches are gaining attention in the pavement industry as the Nuclear Density Gauge (NDG) testing becomes less suitable due to safety, regulatory, and cost concerns.

The Lightweight Deflectometer (LWD) is a portable device that can be utilized to directly measure the surface deflection of unbound layers and then calculate the modulus in the field. However, the resilient modulus of geomaterial is influenced not only by the moisture content (MC) at the time of compaction, but also MC at the time of testing, which may be up to few hours after compaction. Therefore, it is imperative to understand how MC changes in the field after placement, so that this effect can be incorporated into the interpretation of the field modulus value.

Hence, a parametric study has been performed using SoilVision's SVFlux analysis package to model the variation of soil moisture profile with depth versus time as a function of environmental factors and soil type. The SVFlux finite element modeling software simulates the coupled heat and vapor fluxes and estimates the evaporation using the modified Penman method. Gitirana (2004) validated the SVFlux results against experimental results from sand column tests performed by Wilson (1994).

This study was a part of the TPF-5(285) pooled fund study "Standardizing Lightweight Deflectometer Modulus Measurements for Compaction Quality Assurance" conducted by the University of Maryland-College Park with the support of Federal Highway Administration (FHWA), Maryland, Florida, Virginia,

Minnesota, Missouri, North Carolina, South Carolina, and New York state Department of Transportation (MD SHA, FDOT, VDOT, MDOT, MoDOT, NCDOT, SCDOT, and NYSDOT respectively).

The key objectives of this study are to (1) understand the physical process of evaporation from the soil, (2) obtain the moisture loss profile for different soil types and investigate the environmental factors affecting it by performing sensitivity analyses, (3) compare the measured MC using water content sensors in a large-scale test pits with the simulation results for validation purposes, and (4) demonstrate the effect of drying on the LWD measured modulus in a practical field situation.

1.2. Literature review

Water evaporation from soil has been widely investigated in some fields of studies such as agricultural, geotechnical engineering, and mineral industry (Faure and Coussot, 2010). For instance, there are several numerical, laboratory, and field studies to evaluate the performance of soil covers during drying (Khire et al, 1997, Choo and Yanful, 2000, and Yanful et al, 2002).

Prediction of vapor flux across the soil surface is important for many problems in geotechnical engineering. The rate of evaporation from an unsaturated medium depends on not only the climatic conditions but also the soil properties (Wilson et al, 1993).

Faure and Coussot (2010) and Han and Zhou (2013) provide valuable reviews of the physical process of drying in the soil. Generally, three stages are identified as the governing processes of drying in a porous material:

(1) During the first stage the evaporation happens at the material surface and is equal to the potential evaporation rate, which is mostly controlled by atmospheric

parameters such as wind speed and temperature. The available water on the surface is limited to the transported water due to capillary forces.

(2) As the surface moisture decreases, a falling rate period begins. At this stage, a thin dry section forms at the material surface, shifting the evaporation zone to the subsurface. The drying rate is affected by an equilibrium between capillary forces and water flow which is controlled by soil properties.

(3) As the dry surface penetrates the material, drying is mostly controlled by diffusion of water vapor in the dry section with a very low or constant rate. Since both stage two and three happen in the subsurface, they are sometimes considered as one stage.

Penman (1948) developed a method for calculating potential evaporation that only requires routine weather parameter such as air temperature, relative humidity, net radiation, and wind speed. However, the method calculates the evaporation from a free water surface which is an over estimate for the actual unsaturated soil surface.

Wilson (1990) presented a modified Penman approach to calculate the actual evaporation (Wilson-Penman method). He developed a theoretical model based on the coupled heat and mass transfer equations to estimate the evaporation rate from the soil surface (Wilson et al, 1994). Dalton's Law was utilized to determine the evaporation rate from the soil surface based on suction. The water flow and vapor diffusion were explained using Darcy's Law and Fick's Law in addition to the conductive and latent heat fluxes. Then he validated the coupled model with data measured from two columns of sand in an evaporation test. The actual evaporation rates from both sand columns were roughly equal to the potential evaporation rate for the first 3 or 4 days, consistent with the stage one drying phase (Wilson et al, 1994).

Recently Han and Zhou (2013) conducted a numerical simulation to evaluate the dynamics of soil water evaporation by means of coupled heat and water transfer

model. Their simulations considered: (1) water and vapor transfer due to pressure head and temperature gradients, (2) heat transfer in the soil due to conduction, (3) sensible heat convection by water and vapor flow, and (4) movement of latent heat due to vapor diffusion were encompassed in the model. A soil column drying experiment was performed in the lab to calibrate the heat and water transfer model. The results confirm the three stage evaporation phases.

While most studies in the available literature focus on the effect of drying on hydraulic properties and drainage in a soil layer, only a few consider the effect of MC on structural adequacy of compacted soil in unsaturated conditions under traffic loading.

Pacheco and Nazarian (2011) studied the impact of MC at the time of compaction and MC at the time of testing by preparing samples at constant density and measuring the modulus using a free-free resonant (FFRC) column test (ASTM C 215). Their study highlights the impact of the difference between MC at the time of compaction and at the time of testing; as the difference between the two MCs increases, the modulus value at the time of testing increases. Therefore, they suggest requiring a tight schedule between the time of compaction and the time of testing. This issue is more prominent for materials with lower optimum MC values. However, the findings from their study have not been extensively validated in the field.

1.3. Organization of the thesis

Chapter 1 provides the incentives and objectives for this thesis along with a brief review on available literature for evaporation from the soil.

Chapter 2 describes the steps to establish a model in SVFlux and presents the results of the sensitivity analysis on three soil types.

Chapter 3 presents a summary of the test pit construction and instrumentation to measure the volumetric water content (VWC) under controlled conditions (from Khosravifar, 2015) and compares these measurements with the results of VWC simulation using SVFlux.

Chapter 4 includes an introduction to the LWD device configuration, the field project descriptions, and soil properties. It then describes the effect of post compaction drying in the field on measured LWD modulus for two subgrades and two base layer soils.

Chapter 5 summarizes the findings regarding the application of MC variation in the field on the modulus-based QA procedure and offers recommendation for future research.

2. Chapter 2: Sensitivity Analysis

The variation of moisture profile with time is modeled using SVFlux™ by SoilVision™ 2009 finite element package for three soil types in this chapter. A parametric study is conducted to evaluate the sensitivity of a modeled soil in terms of moisture loss to each parameter in a short period of time.

The parametric study considers moisture profiles in homogeneous and layered soils in an uncovered state as a function of environmental factors (e.g. air temperature, relative humidity, and wind speed) and soil properties (e.g., soil type, soil water characteristic curve, and saturated hydraulic conductivity).

The results from the parametric study will help to identify which soils have significant versus negligible drying over various short-term time periods.

2.1. SVFlux software

The SoilVision was first established and announced in 1997 to address the demand for implementation of unsaturated soil mechanics for practical problems. The SVFlux application is a part of the the SVOffice analysis package by SoilVision Systems, Inc. The SVFlux package, developed in 2001, solves the partial differential equations (PDE) for groundwater flow using finite element analysis. The software is commonly used for seepage problems in the hydrology field. It is designed to analyze both saturated and unsaturated flow in steady-state or transient time conditions (Lu, 2015).

The theoretical method of calculating the rate of evaporation from an unsaturated soil surface was developed by Wilson (1990) based on the Dalton's Law and a modified Penman's approach. Darcy's Law and Fick's Law are used to define the water and vapor flow in the saturated/unsaturated soil layer. The system of equations proposed by Wilson (1990) are presented below:

Evaporation:

Equation 2-1

$$E = f(u)(e_s - e_a)$$

E : Vertical vapor flux into the atmosphere (mm/day),

$f(u)$: A function depending on wind speed, surface roughness and atmospheric stability,

e_s : The vapor pressure at the soil surface (kPa),

e_a : The vapor pressure in the air above the soil surface (kPa).

Moisture flow:

Equation 2-2

$$\frac{\partial h_w}{\partial t} = C_w^1 \frac{\partial}{\partial y}\left(k_w \frac{\partial h_w}{\partial y}\right) + C_w^2 \frac{\partial}{\partial y}\left(D_V \frac{\partial P_V}{\partial y}\right)$$

Heat flow:

Equation 2-3

$$C_V \rho_S \frac{\partial T}{\partial t} = \frac{\partial}{\partial Y}\left(\lambda \frac{\partial T}{\partial t}\right) - L_V \left(\frac{P + P_V}{P}\right) \frac{\partial}{\partial Y}\left(D_V \frac{\partial P_V}{\partial Y}\right)$$

k_w : The coefficient of permeability as a function of matric suction,

C_w^1 , C_w^2: The coefficients associated with consolidation due to liquid flow,

D_V : Vapor diffusion,

P : Total pressure in the bulk air phase (kPa),

P_V : The actual vapor pressure within the pore air (kPa),

h_w : Total hydraulic head (m),

Y : Vertical position (m),

ρ_W : Density of liquid water (kg/m^3),

$C_V \rho_S$: Volumetric specific heat,

T : Temperature (°C),

λ : The thermal conductivity (W/m °C),

L_V : Latent heat of vaporization (J/kg).

The moisture and heat flow equations are nonlinear with respect to head, position, and time, which makes the solution of the equations challenging. Wilson (1990) successfully obtained the solution using an explicit finite difference scheme. He designed a 1D finite element suite named "Flux" to compare the measurements from a drying sand column to the numerical solution. Good agreement was observed between the measured and computed values for water content and soil temperature.

Gitirana (2004) used the FlexPDE solver in SVFlux to perform a preliminary evaluation of the Wilson (1990) results (SVFlux Verification Manual). The SVHeat package is also required to model the fully coupled water and heat flow through the soil. However, for the short time span of interest for this study, uncoupled evaporation simulation using SVFlux was determined to be sufficient.

Generating a numerical model requires taking the following steps:

1. Create model and define settings: The dimensions of the model (1D, 2D, or 3D), transient or steady analysis type, unit system (SI or Metric), time and length units, start and end time for the analysis, and the initial and maximum time increment are set at this step. The models in this study were generated for 1D vertical transient flow.
2. Input model geometry: The general geometry data (soil depth for 1D) is entered at this step by drawing or inserting polygons.
3. Define initial conditions: Initial conditions for transient models specify the starting point as the finite element solution of the partial differential equations. The initial condition entered for SVFlux are the pore water pressure or

hydraulic head for hydrostatic condition. An initial pressure of zero characterizes a phreatic surface, whereas the pressure values greater than zero represents at saturation condition to start. Pressure values less than zero correspond to unsaturated initial conditions.

4. Define boundary conditions: SVoffice offers a variety of boundary conditions (BC) for different situations. The following are the common BCs used for SVFlux modeling:
    a. Flux BC: A unit flux (q) can be assigned to pass through a boundary. The prescribed flux values can be varied with time for transient analysis using data BC or an expression.
    b. Zero flux BC: A special case of the Flux BC corresponding to impermeable/insulating boundaries.
    c. Climate: To apply the precipitation, snow cover, potential evaporation, actual evaporation, transpiration, and other atmospheric conditions, a Climate Manager dialog is used. Then the Climate BC is applied to the boundary that is exposed to the atmosphere.

       The Evaporation Dialog from Climate Manager is only applied for the purpose of this study, since compaction is performed in the absence of heavy precipitation and vegetation. Evaporation properties include the selection of potential evaporation and actual evaporation calculation methods. Potential evaporation can be input as constant, via an expression, using the Penman (1948) method, or as data tables. Actual evaporation maybe set equal to the potential evaporation or determined from the Modified Wilson-Penman (1994), Modified Wilson Limiting Equation (1997), or Modified Wilson Empirical Equation (1997) methods.

       Evaporation properties dialog also requires the input of air temperature, air relative humidity, net radiation, and wind speed data

which can also be quantified as constants, expressions, or tables of data.

5. Assign material properties: The material properties in SVFlux include saturated hydraulic conductivity, unsaturated hydraulic conductivity calculation method, Soil Water Characteristic Curve (SWCC) method, saturated volumetric water content, specific gravity, etc. Material properties are managed through Material Manager dialog, then assigned to the polygon regions using Region Properties dialog. In this study, the Fredlund and Xing approach is used to characterize the SWCC and the Modified Campbell theoretical method is used to estimate the unsaturated hydraulic conductivity.
6. Determine solver outputs: The output variables are specified using the Output Manager dialog. The results can be VWC, pore water pressure, matric suction, degree of saturation, pressure head, etc. The output increment can be adjusted based on the start, end, and maximum increment times for the analysis. The software can also display a real-time plot of the results while running. The main outputs of interest for this study are VWC and gravimetric water content (GWC).
7. Run the model: By clicking the analyze button, the FlexPDE solver will start solving the model and preview graphs of outputs to show the progress.

2.2. Soil characterization

Three types of soils from Yanful and Choo (1997) were used to simulate the variation of moisture profile with time using SVFlux. Table 2-1 includes the hydraulic properties of the soils. The SWCCs and geotechnical properties are presented by Machibroda et al (1993) and Yanful and Choo (1997).

Table 2-1. Initial hydraulic properties of the soils (after Yanful and Choo, 1997).

	Coarse sand	Fine sand	Clay
Estimated unsaturated hydraulic conductivity [m/s]	modified Campbell method		
Saturated hydraulic conductivity [m/s]	2.00E-04	1.00E-05	6.70E-11
Potential evaporation [mm/day]	6.5	-	-
Initial MC [%]	17	26	30
Suction [kPa]	1	1	>100

All three models simulate 1D vertical transient flow over a soil depth of 30 cm (11.8 in). The simulation analysis period is 24 hours for all models. The outputs of interest are the amount and depth of drying in the soil.

The boundary conditions for all models were defined as the Climate BC on the top and Zero flux BC in the bottom. Potential evaporation was estimated based on the initial evaporation rate for each soil. Air temperature and relative humidity was matched to the environmental chamber for the first day (Yanful and Choo, 1997, Figure 4- Figure 9). The initial water content distribution is assumed uniform throughout the depth.

Based on the preliminary analysis, the clay soil experienced significant drying over the first 5 cm (~2 in). Therefore, a finer mesh for output variables was employed to capture the water content close to the surface.

2.3. Results

Figure 2-1 presents the of SVFlux gravimetric MC results for the fine sand soil. The initial MC was 26% and assumed to be uniform in depth. The amount of drying after 1,5, and 10 hours are about 0.6, 1.3, 2 percentage points respectively, with the maximum drying happening on the soil surface. The final surface MC is reduced to 22.6% after 24 hours. The depth of drying remained at 10 cm (~4 in) below the surface after the first 10 hours, then progressed to 20 cm (~8 in) after a day.

Water content profile for the coarse sand is exhibited in Figure 2-2 with an initial MC of 17%. The amount of surface drying in this model is 0.26, 1.2, 2.4 and 5 percentage points after 1, 5, 10, and 24 hours respectively. The rate of drying is higher compared to the fine sand; this would be expected given the lower suctions in the coarser soil. Moreover, the initial MC should also be considered as the fine sand soil column model starts with a higher initial MC, therefore, more water is available near the surface to evaporate. The drying front progressed deeper into the coarse sand layer comparing to fine sand soil. The depth of drying is 15 cm (~6 in) after the first 10 hours, ultimately increasing to 23 cm (~9 in) after 24 hours. This could be due to both evaporation and downward moisture flow through the soil.

Figure 2-3 shows the drying in the clay soil model. The initial MC for the clay is 30%, which is significantly higher than fine and coarse sand material. The amount of drying experienced on the surface is 2.2, 5, 7.7, and 10.1 percentage points after 1, 5, 10, and 24 hours respectively. However, these amounts reduce significantly to 0.5, 1.1, 1.7 and 2.3 percentage points at a depth of 2.5 cm (~1 in) below the surface, indicating that the evaporation is limited to the top of the soil with little transport of water from beneath the surface zone. Moreover, the depth of drying remained constant at about 5 to 8 cm (~2 to 3 in) below the surface, which is shallow compared to the fine and coarse sand models.

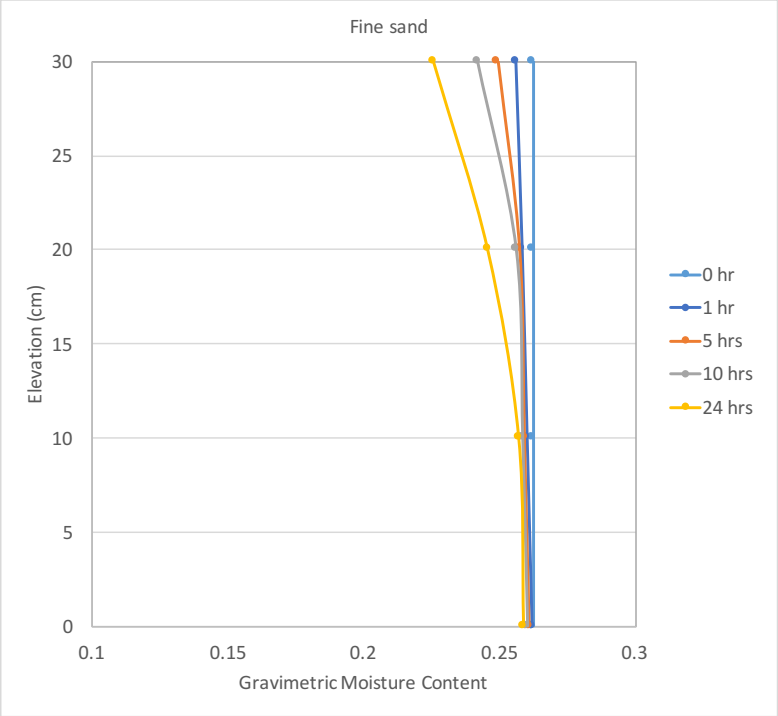

Figure 2-1. MC profile during 24 hours, fine sand soil.

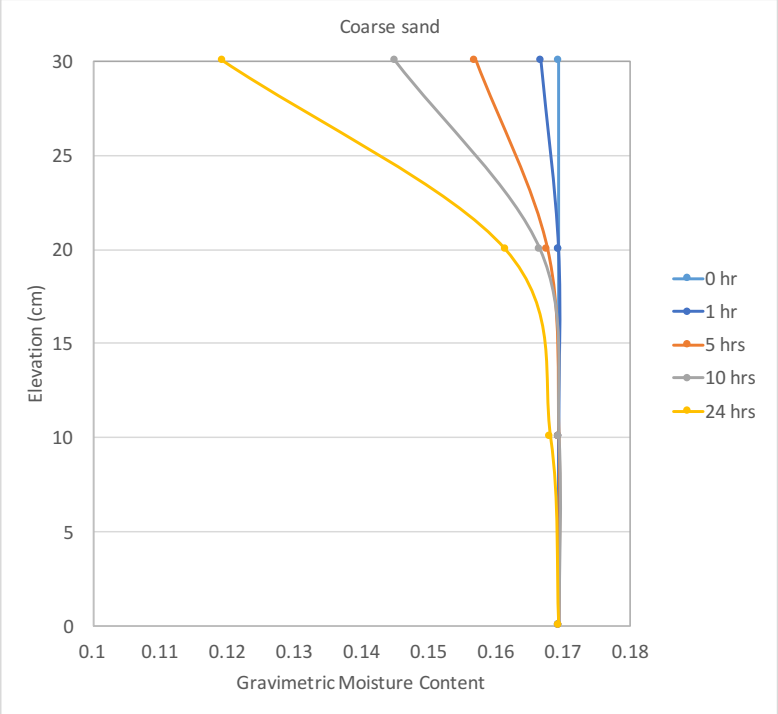

Figure 2-2. MC profile during 24 hours, coarse sand soil.

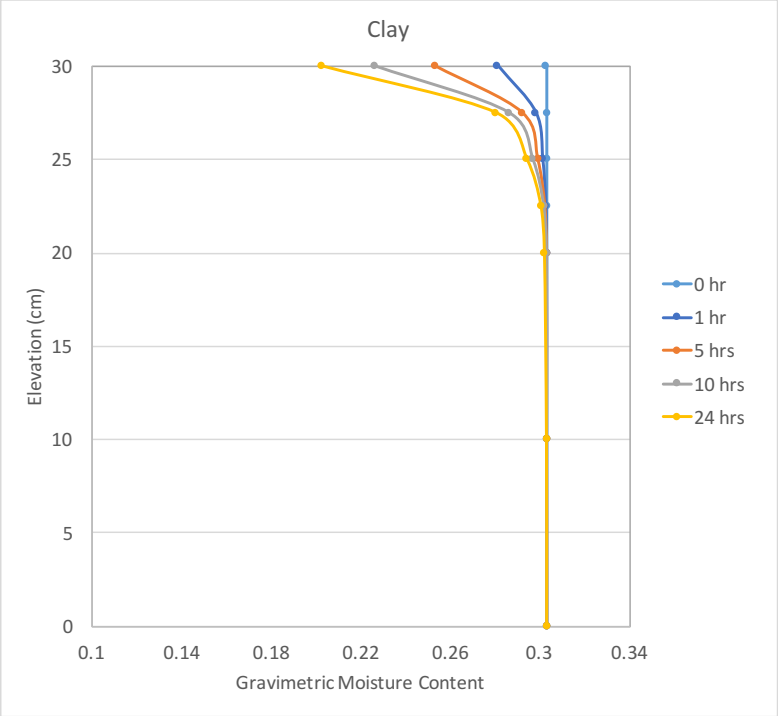

Figure 2-3. MC profile during 24 hours, clay soil.

2.4. Sensitivity analysis for fine sand soil

A parametric study is performed using SVFlux to evaluate the sensitivity of soil MC at different depths to environmental factors such as air temperature, relative humidity, and wind speed. The effect of sun shine ratio was found to be minimal while keeping the temperature constant.

2.4.1. Sensitivity to temperature

The air temperature at the Climate Manager dialog was varied between 10 to 38 ºC while keeping other factors constant for the fine sand soil model. Drying (changes in gravimetric water content) is predicted at the surface and and depths of 5, 10, 15, 20, 25, 30 cm (~2, 4, 6, 8, 10, 12 in respectively). Figure 2-4 presents the results for 5, 7, 12, 16 and 24 hours into the analysis. Moisture loss in the fine sand model increases with increasing temperature. The effect of temperature on drying is more prominent in the first 15 cm (~6 in) of the soil column.

Figure 2-5 demonstrates the sensitivity of MC to initial temperature as the moisture loss per temperature change versus time for the fine sand soil. Y-axis is calculated as the slope of MC loss (percentage points) versus temperature. The sensitivity to temperature decreases on the soil surface with time, as the drying front penetrates below the surface. On the other hand, the sensitivity increases with depth up to 20 cm (~8 in) with time. For this soil type, the MC is relatively insensitive to initial temperature at depths greater than 20 cm. This graph can be used to estimate the amount of drying change per temperature change for up to 24 hours after material placement in the field.

A)

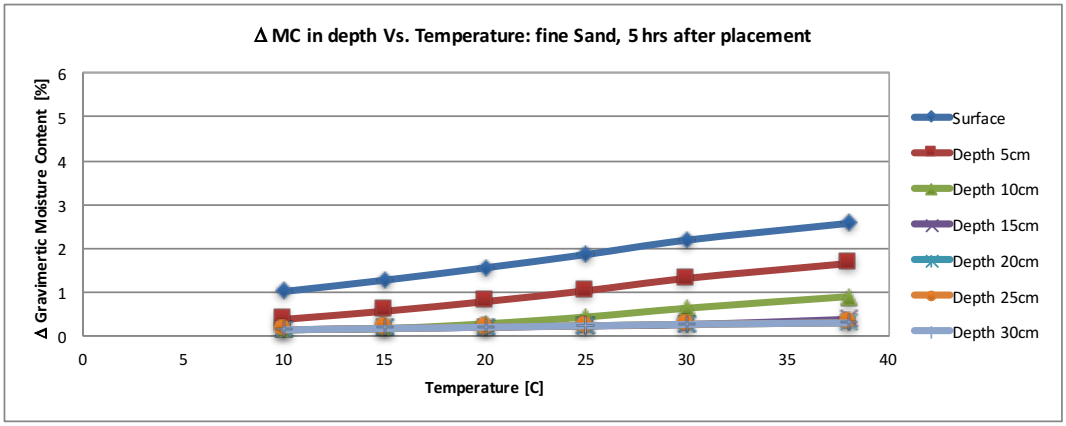

B)

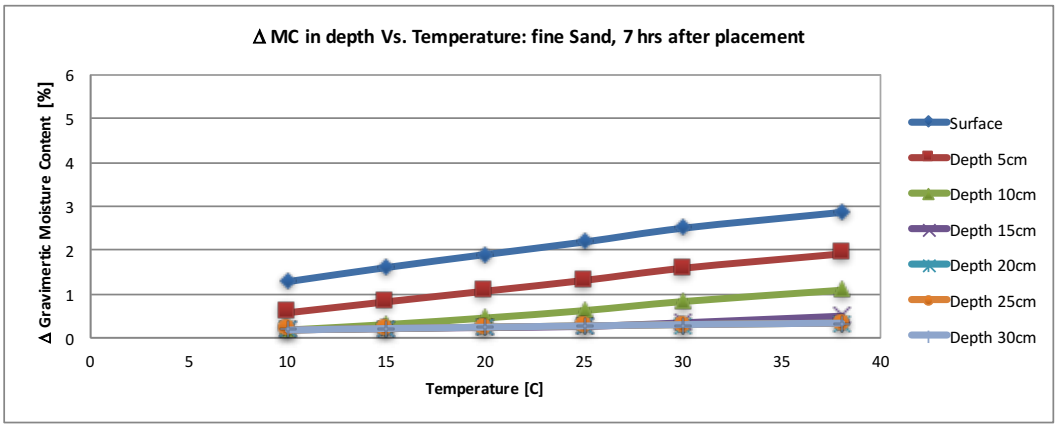

C)

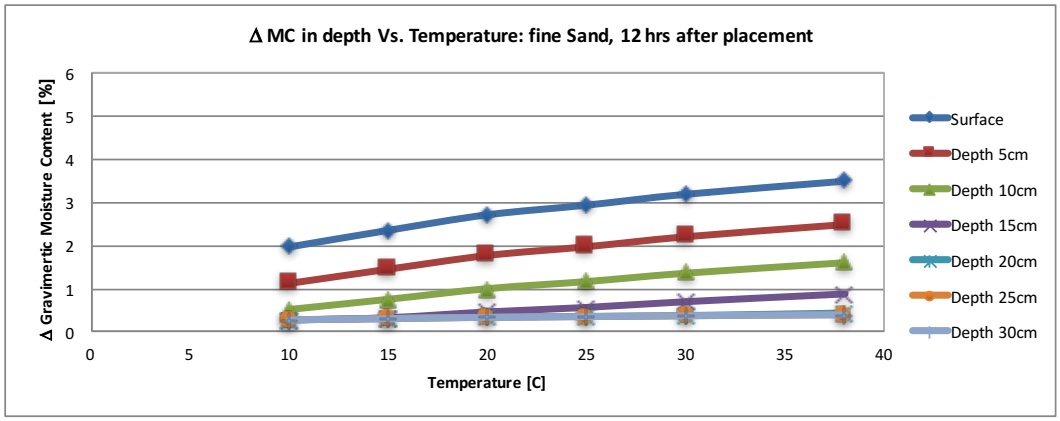

D)

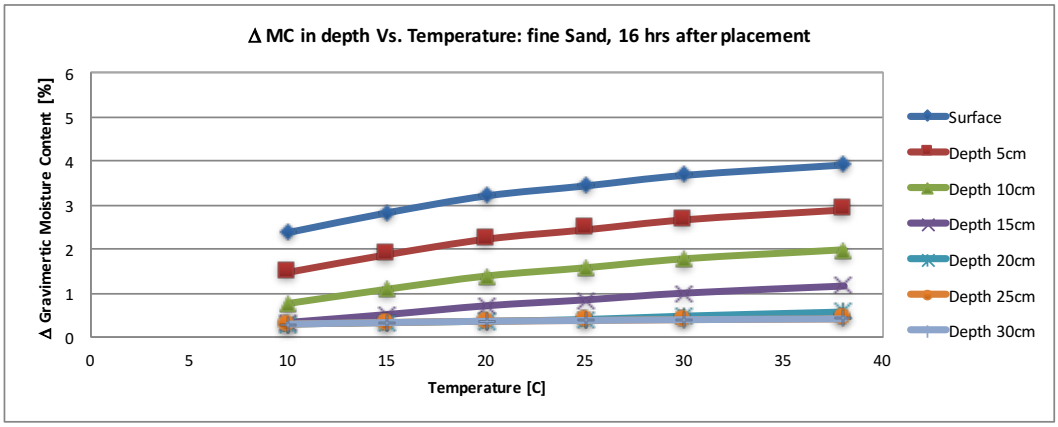

E)

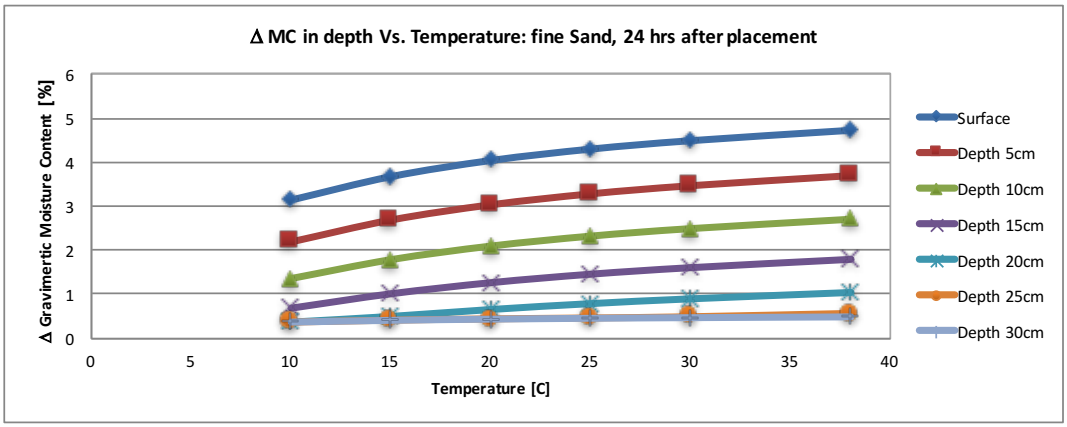

Figure 2-4. Simulated %MC loss versus temperature at different depth for fine sand soil, (A) 5 hours, (B) 7 hours, (C) 12 hours, (D) 16 hours and (E) 24 hours after compaction.

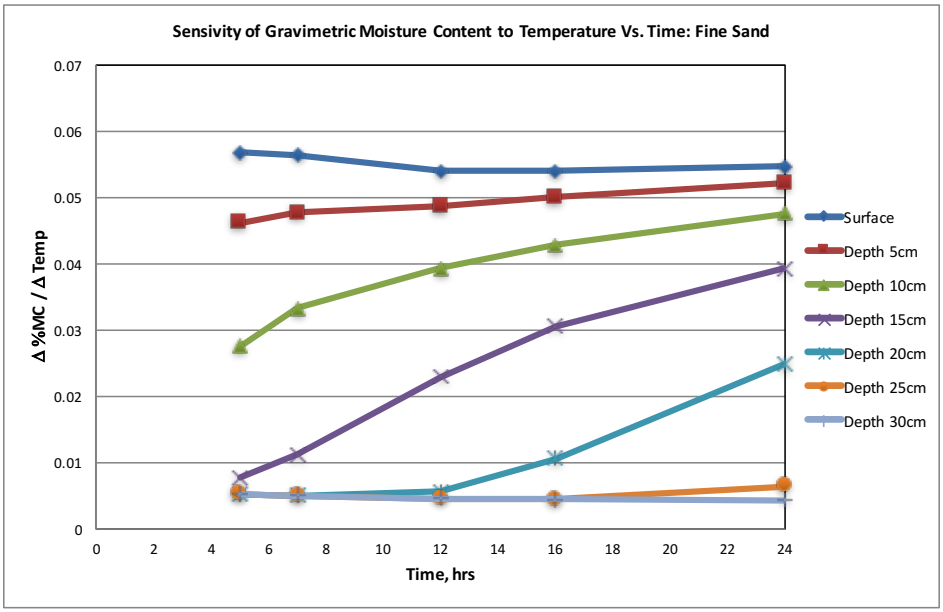

Figure 2-5. Sensitivity of MC to temperature versus time at different depth for fine sand.

2.4.2. Sensitivity to wind speed

Similar to temperature, the wind speed is changed between 3 to 80 km/hr while keeping other climate factors constant. Moisture loss is graphed versus wind speed at different depths in Figure 2-6 for the fine sand soil model.

The drying in the fine sand soil increased as the wind speed increased up to 40 km/hr and remained constant for higher speeds. However, a wind speed of more than 40 km/hr (~25 mph) may not normally be experienced in the field. It can also be noticed that the wind speed does not affect the moisture loss in fine sand soil below the 20 cm (~8 in) depth from the surface

The sensitivity of MC loss to wind speed is presented in Figure 2-7. Y-axis is calculated as the slope of MC loss (percentage points) versus wind speed. This sensitivity is lower than the sensitivity to temperature by a factor of 3. Moreover, the sensitivity of the top 5 cm (~2 in) of the soil does not change with time, and as the drying front progresses into the soil layer, more change in drying is observed with increase in wind speed over the depth range of 10 to 20 cm.

A)

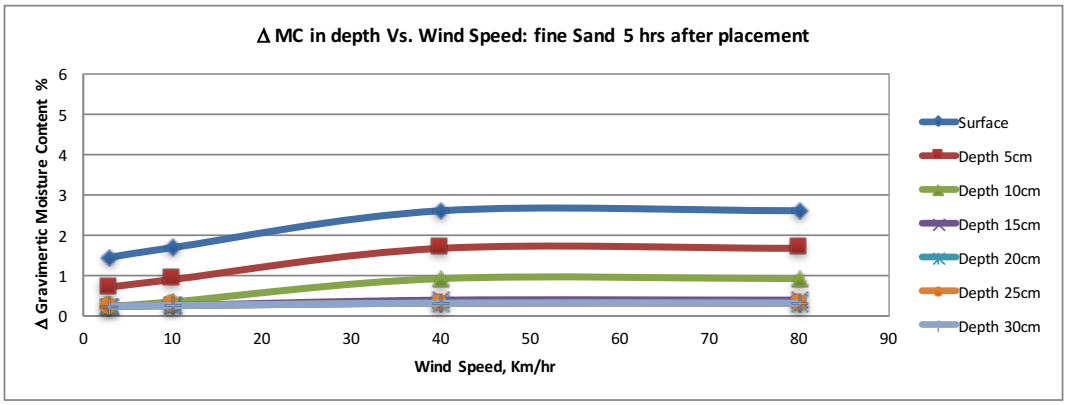
Δ MC in depth Vs. Wind Speed: fine Sand 5 hrs after placement
Δ Gravimertic Moisture Content %
0
1
2
3
4
5
6
0
10
20
30
40
50
60
70
80
90
Wind Speed, Km/hr
Surface
Depth 5cm
Depth 10cm
Depth 15cm
Depth 20cm
Depth 25cm
Depth 30cm

B)

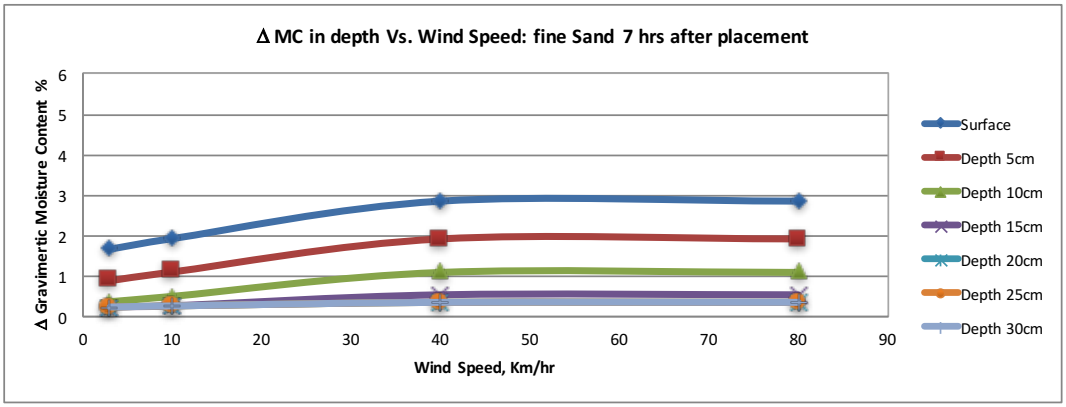
Δ MC in depth Vs. Wind Speed: fine Sand 7 hrs after placement
Δ Gravimertic Moisture Content %
0
1
2
3
4
5
6
0
10
20
30
40
50
60
70
80
90
Wind Speed, Km/hr
Surface
Depth 5cm
Depth 10cm
Depth 15cm
Depth 20cm
Depth 25cm
Depth 30cm

C)

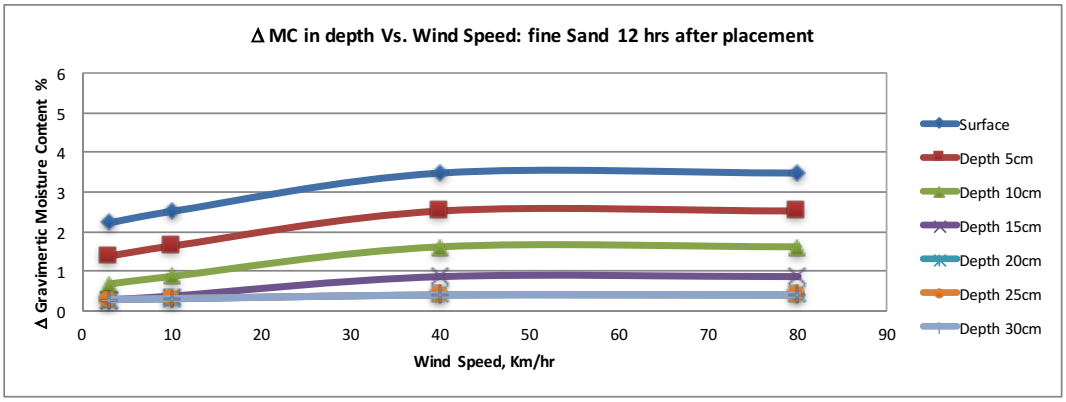
Δ MC in depth Vs. Wind Speed: fine Sand 12 hrs after placement
Δ Gravimertic Moisture Content %
0
1
2
3
4
5
6
0
10
20
30
40
50
60
70
80
90
Wind Speed, Km/hr
Surface
Depth 5cm
Depth 10cm
Depth 15cm
Depth 20cm
Depth 25cm
Depth 30cm

D)

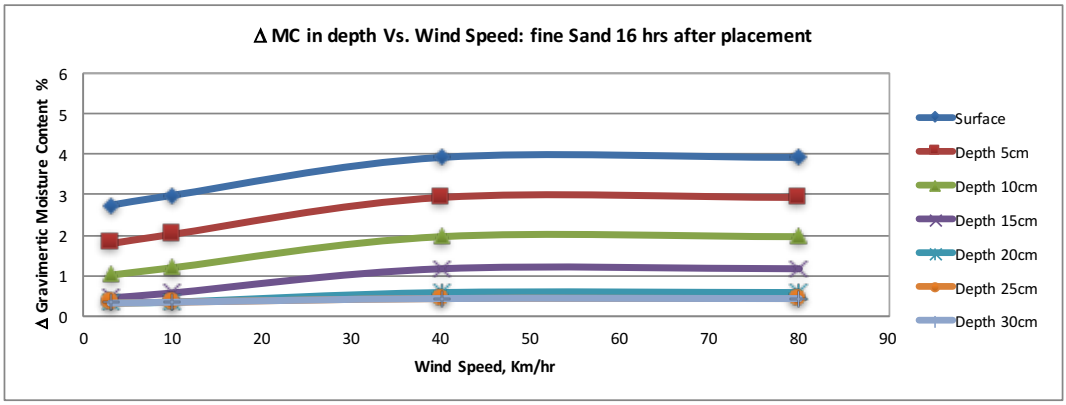

E)

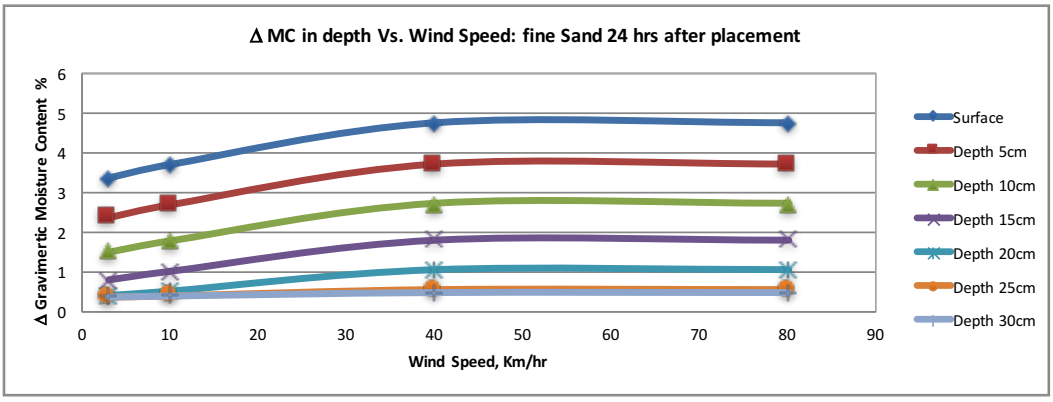

Figure 2-6. Simulated %MC loss versus wind speed at different depth for fine sand soil, (A) 5 hours, (B) 7 hours, (C) 12 hours, (D) 16 hours and (E) 24 hours after compaction.

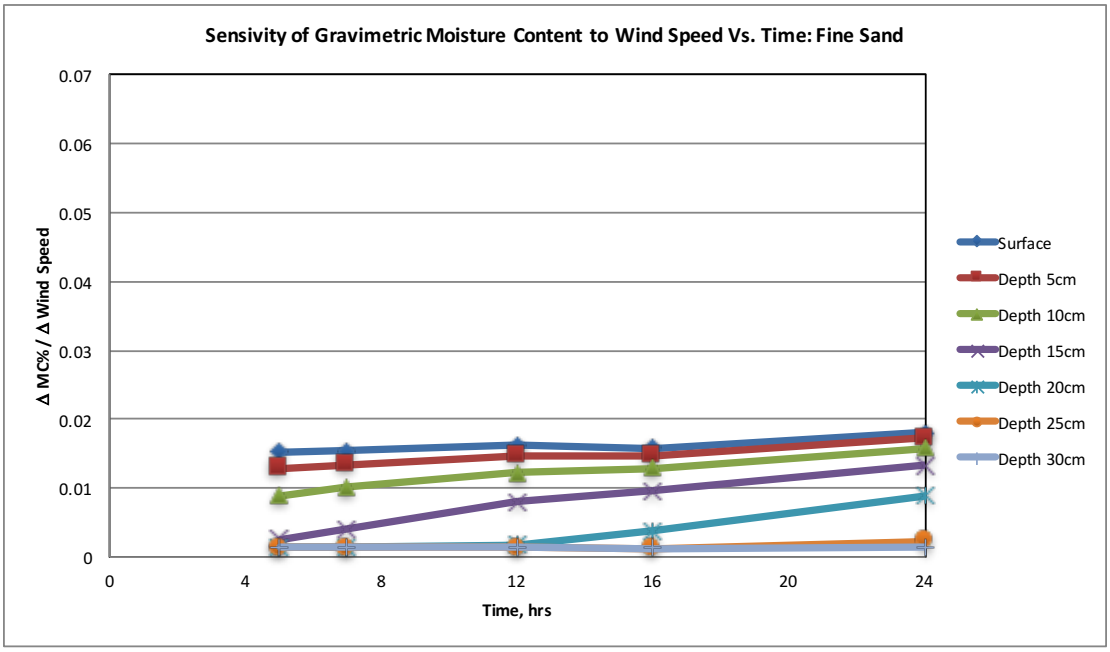

Figure 2-7. Sensitivity of MC to wind speed versus time at different depth for fine sand.

2.4.3. Sensitivity to relative humidity

Relative humidity (RH) is defined as the percentage of water vapor to the amount needed for saturation at the same temperature. Keeping the temperature and wind speed constant, the RH was varied between 10% to 90%. The changes in gravimetric moisture content is graphed versus %RH at different depth and time spans (Figure 2-8). Moisture loss in the fine sand model slightly decreased with increase in the RH. The change in MC under different RHs occur within the depth of 20 cm (~8 in) from the surface during the first 24 hours.

Figure 2-9 demonstrates the slope of MC loss (percentage points) versus RH graph as Y-axis, at different times (X-axis) for fine sand soil. Since there is an inverse relationship between the drying rate and RH, these sensitivity values are negative. In absolute value terms, the sensitivity of MC to RH is less than the sensitivity to temperature by an order of magnitude.

A)

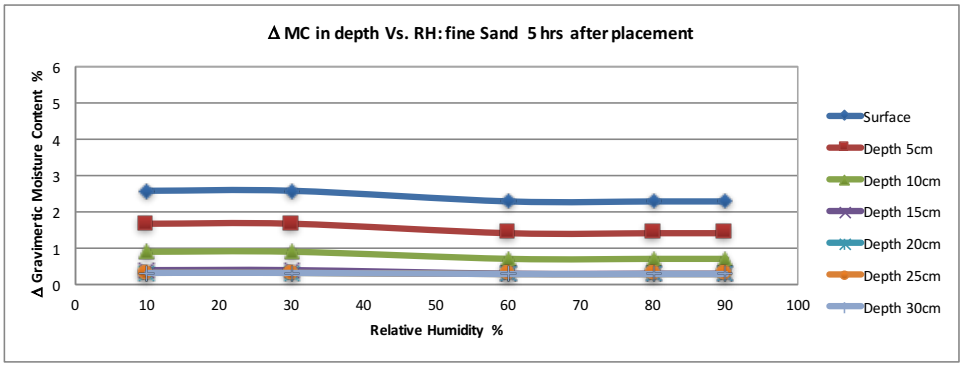
Δ MC in depth Vs. RH: fine Sand 5 hrs after placement
Δ Gravimertic Moisture Content %
Relative Humidity %
Surface
Depth 5cm
Depth 10cm
Depth 15cm
Depth 20cm
Depth 25cm
Depth 30cm

B)

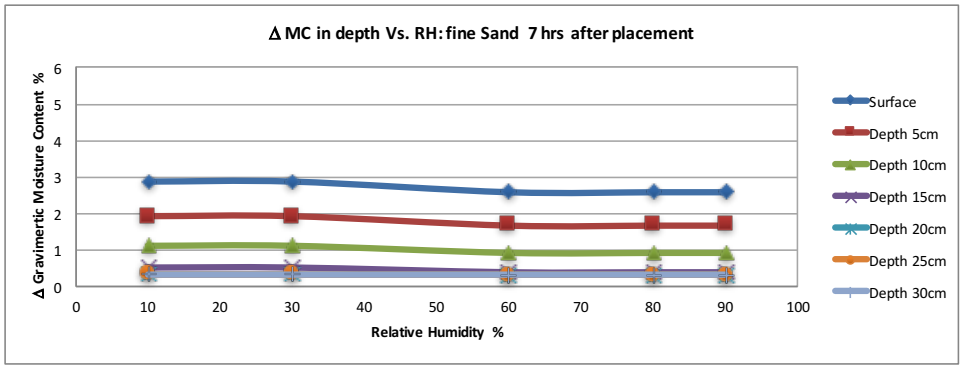
Δ MC in depth Vs. RH: fine Sand 7 hrs after placement
Δ Gravimertic Moisture Content %
Relative Humidity %
Surface
Depth 5cm
Depth 10cm
Depth 15cm
Depth 20cm
Depth 25cm
Depth 30cm

C)

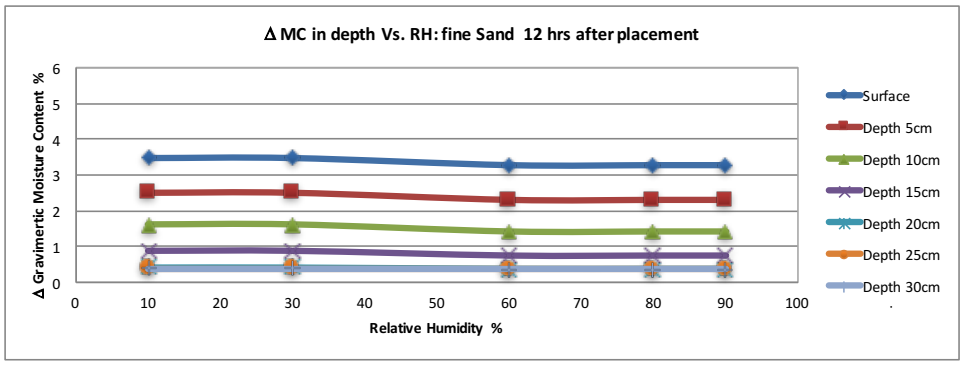
Δ MC in depth Vs. RH: fine Sand 12 hrs after placement
Δ Gravimertic Moisture Content %
Relative Humidity %
Surface
Depth 5cm
Depth 10cm
Depth 15cm
Depth 20cm
Depth 25cm
Depth 30cm

D)

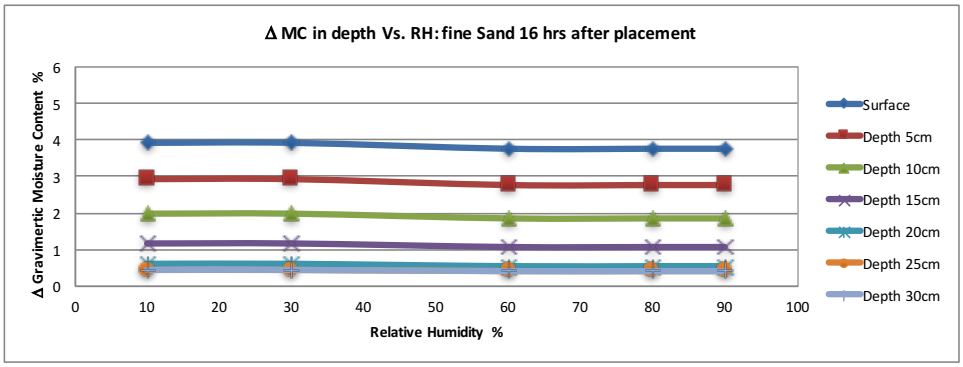
Δ MC in depth Vs. RH: fine Sand 16 hrs after placement
Δ Gravimertic Moisture Content %
Relative Humidity %
Surface
Depth 5cm
Depth 10cm
Depth 15cm
Depth 20cm
Depth 25cm
Depth 30cm

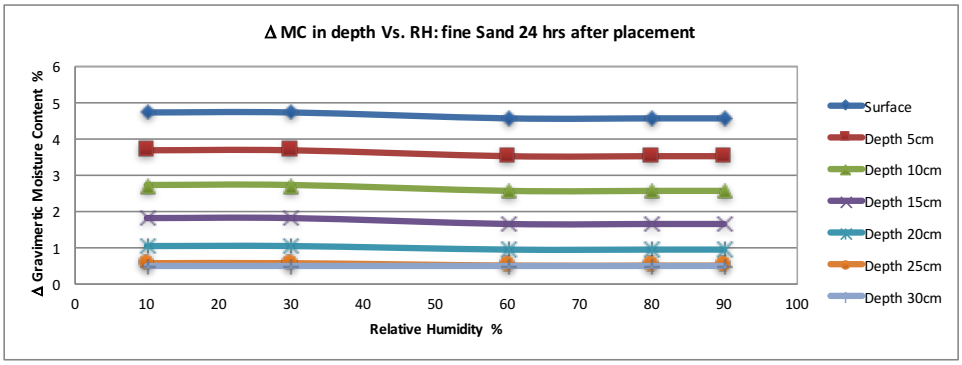

E)

Figure 2-8. Simulated %MC loss versus relative humidity at different depth for fine sand soil, (A) 5 hours, (B) 7 hours, (C) 12 hours, (D) 16 hours and (E) 24 hours after compaction.

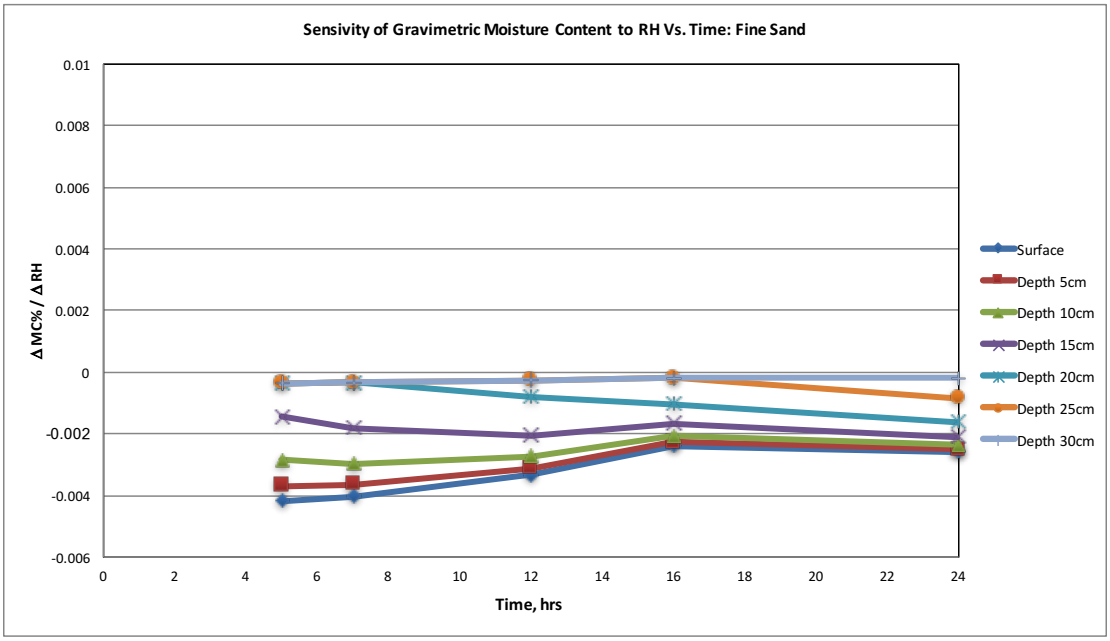

Figure 2-9. Sensitivity of MC to relative humidity versus time at different depth for fine sand.

2.5. Sensitivity analysis for coarse sand soil

Similar to the fine sand soil model, the moisture loss in the coarse sand soil from Yanful and Choo (1997) is modeled by SVFlux. The sensitivity to the atmospheric parameters: temperature, wind speed, and relative humidity are graphed versus time to demonstrate the MC variations at different depths.

2.5.1. Sensitivity to temperature

Figure 2-10 presents the slope of percentage point loss in moisture content per temperature change versus time (sensitivity to temperature) for the coarse sand soil. A decreasing trend in the sensitivity is observed on the soil surface similar to fine sand soil. And as the drying front penetrates the modeled soil column, the trend becomes increasing up to 25 cm (~10 in). For this soil type, the sensitivity to temperature does not change with time below the 25 cm depth.

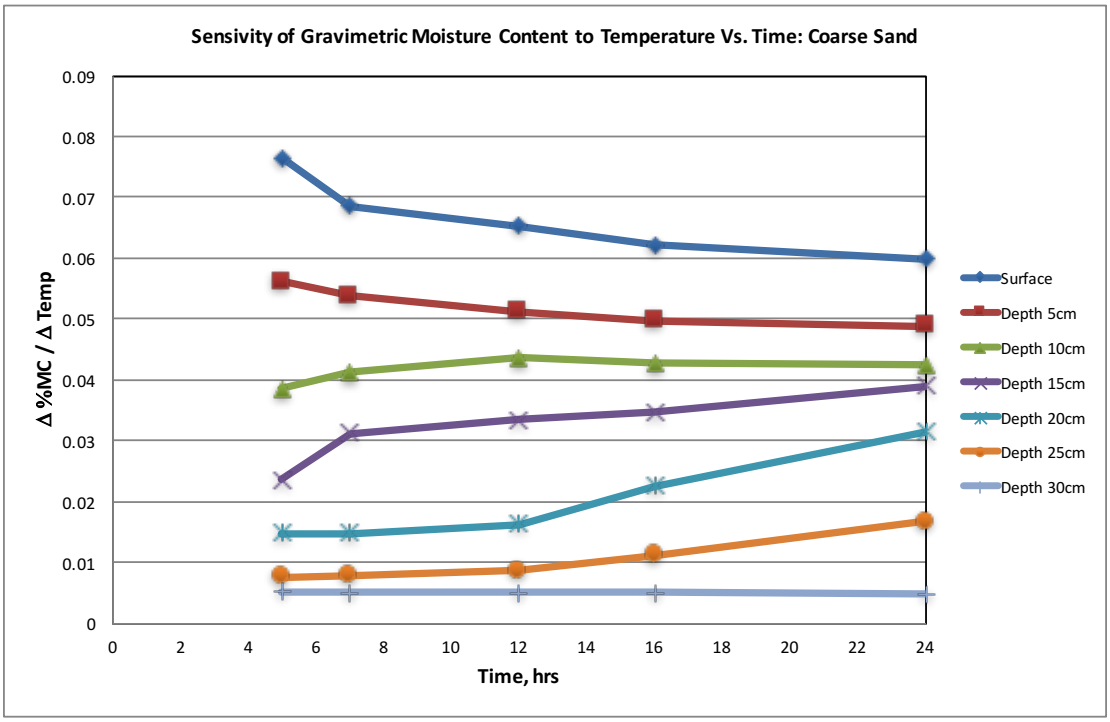

Figure 2-10. Sensitivity of MC to temperature versus time at different depth for coarse sand.

2.5.2. *Sensitivity to wind speed*

Figure 2-11 shows the sensitivity of coarse sand soil to wind speed at each depth. This sensitivity is about half of the sensitivity to temperature with an increasing trend at all depth up to 25 cm. The bottom 5 cm is not sensitive to wind speed during the first 24 hours of drying.

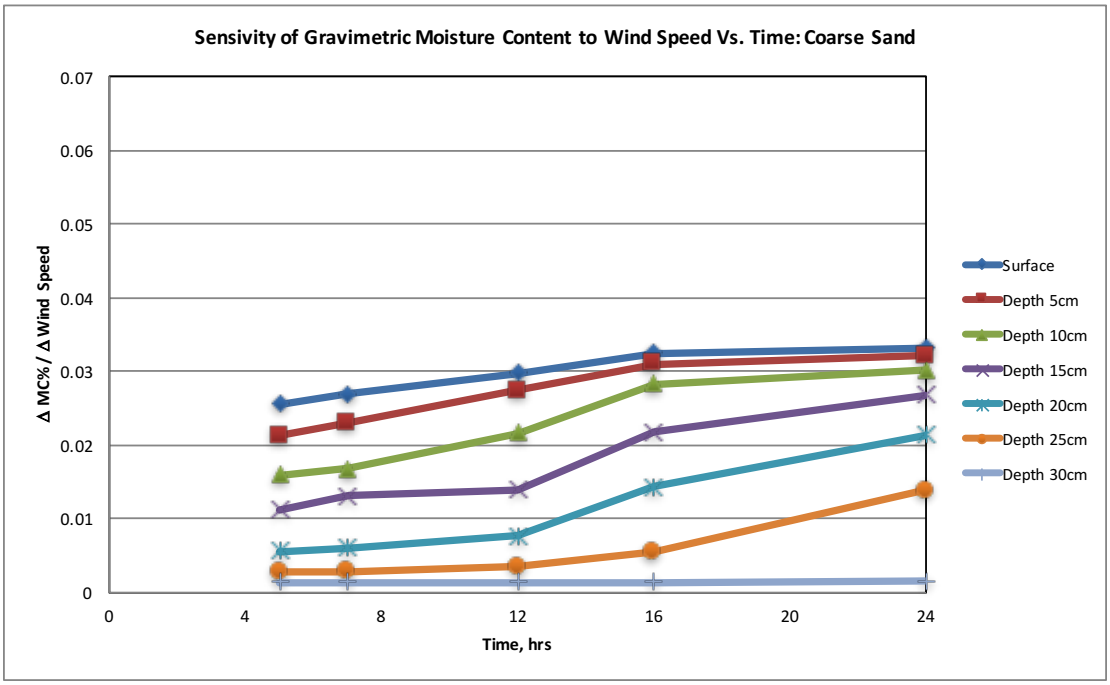

Figure 2-11. Sensitivity of MC to wind speed versus time at different depth for coarse sand.

2.5.3. *Sensitivity to relative humidity*

Figure 2-12 demonstrates the slope of moisture loss per RH change (MC sensitivity to RH) versus time for coarse sand soil. Similar to the fine sand soil, the sensitivity values are negative. The absolute values of sensitivity to RH are less than the sensitivity to temperature values by an order of magnitude. The magnitude of sensitivity is decreasing with time at the surface layers, and at the depth of 15 to 25 cm (6 to 8 in) this trend is reversed. The sensitivity to RH is very low and close to zero at the final 5 cm (2 in) of the soil column.

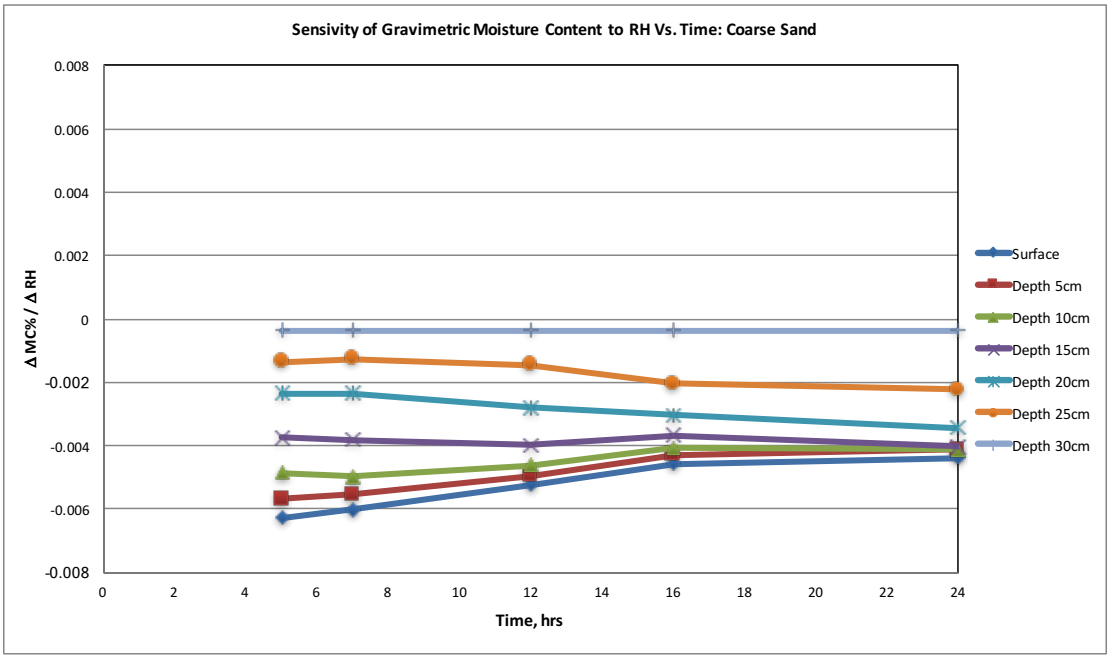

Figure 2-12. Sensitivity of MC to relative humidity versus time at different depth for coarse sand.

2.6. Sensitivity analysis for clay soil

The sensitivity to temperature, wind speed, and RH are investigated by varying each parameter and keeping all other parameters constant for the clay soil. Then the slope of change in MC to the change in every parameter is graphed versus time, similar to the sand soils.

2.6.1. Sensitivity to temperature

Figure 2-13 shows the sensitivity of the clay soil to the initial temperature versus time for the first 24 hours after compaction. The sensitivity on the top 5 cm (2 in) is increasing with time, and remains constant in the depth below that. The sensitivity to temperature in the clay soil surface is approximately 30% of the sensitivity in fine sand and about 25% of it in the coarse sand soil.

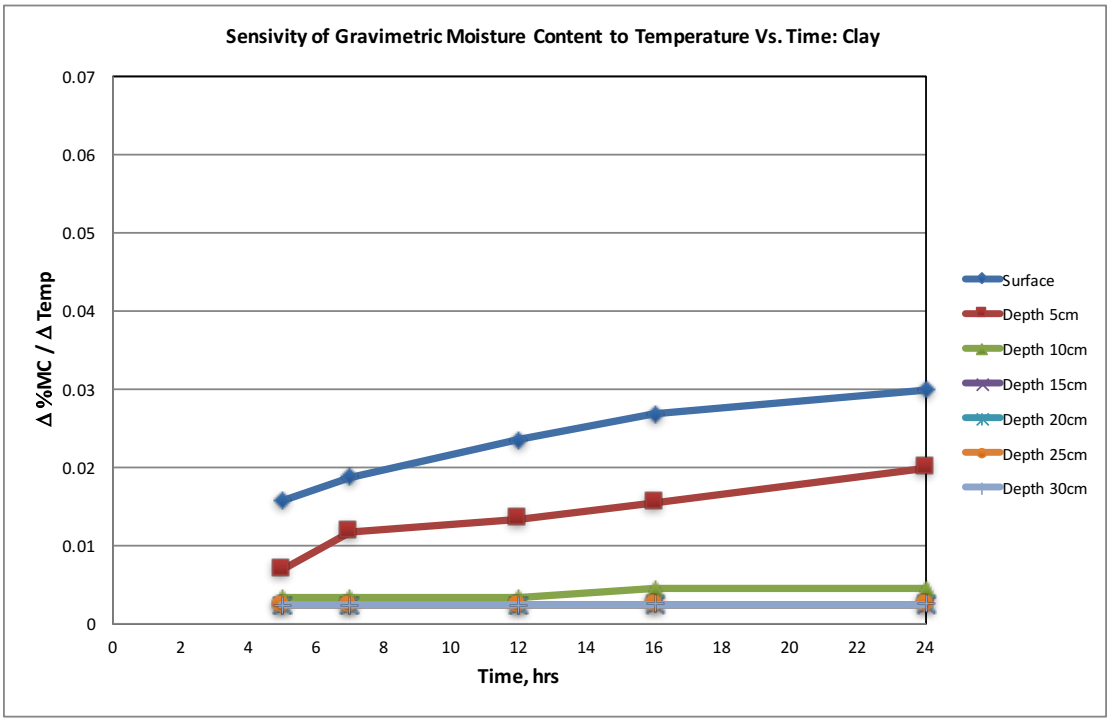

Figure 2-13. Sensitivity of MC to temperature versus time at different depth for clay soil.

2.6.2. *Sensitivity to wind speed*

Figure 2-14 presents the sensitivity to wind speed versus time for the modeled clay soil in SVFlux. Generally, the sensitivity slightly increases with time for the first 5 cm (2 in), while remaining constant and close to zero below that depth. The sensitivity to wind speed is about half of that value for temperature in this soil type.

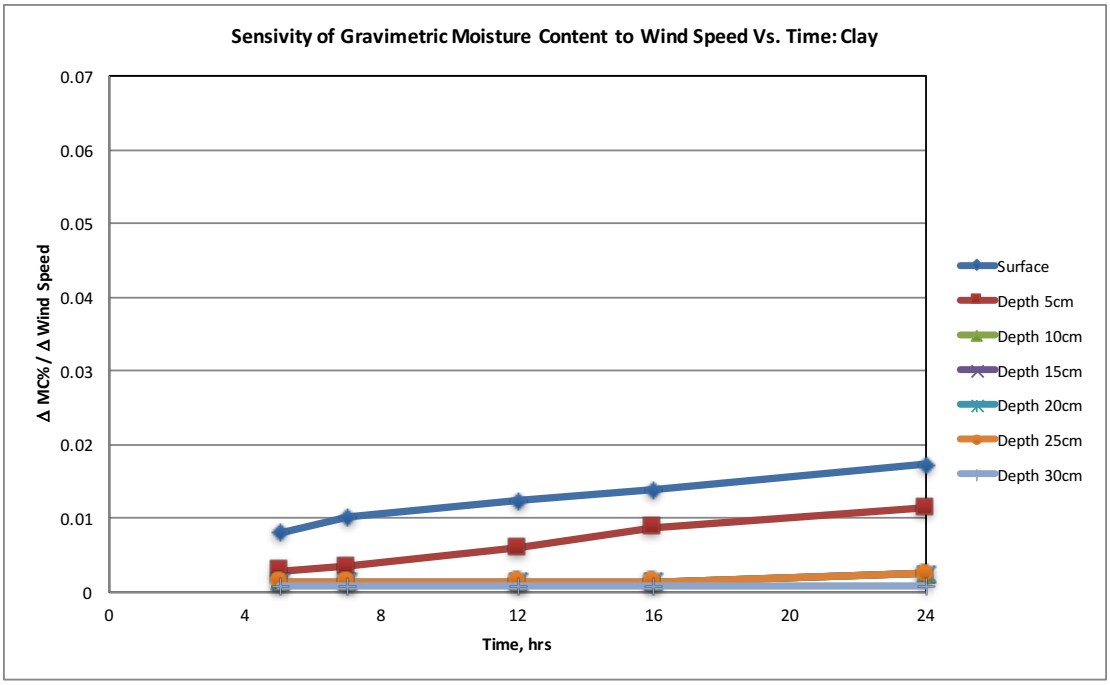

Figure 2-14. Sensitivity of MC to wind speed versus time at different depth for clay soil.

2.6.3. *Sensitivity to relative humidity*

The sensitivity to RH is presented in Figure 2-15 for the first 24 hours for clay soil. This sensitivity value is very low comparing to fine and coarse sand soils and its magnitude is slightly decreasing with time only for the first 5 cm.

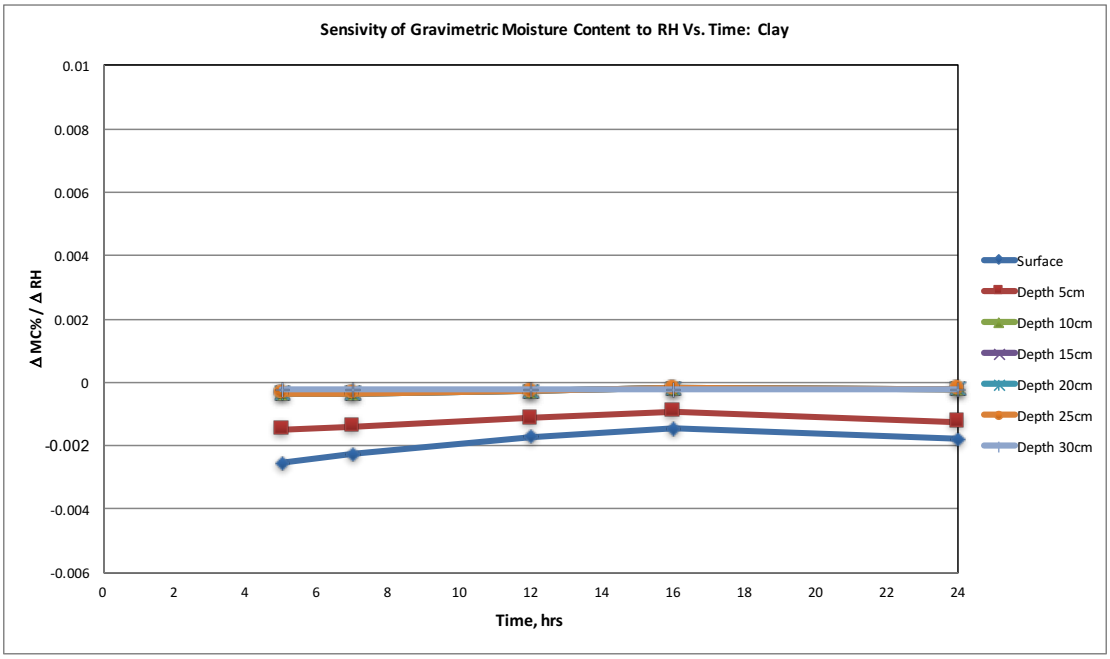

Figure 2-15. Sensitivity of MC to relative humidity versus time at different depth for clay soil.

2.7. Conclusions

SVFlux was used to model the moisture loss vs. depth during drying for the three soil types originally studied by Yanful and Choo (1997). A time span of 24 hours after material placement is considered for practical implementation. The amount and depth of drying is demonstrated and compared for the three soil types. As expected, the coarse sand soil experiences more drying and greater depth of dry front penetration as compared to the fine sand and clay soils. The depth of drying for the clay soil is the minimum.

Additionally, a limited parametric study was conducted to evaluate the sensitivity of MC in the three soil types to the main atmospheric parameters: temperature, wind speed, and relative humidity. The change in moisture content was modeled in SVFlux by fixing all but one of the parameters. The sensitivity to sun shine ratio was found to be insignificant when keeping the temperature constant.

All three soils proved to be most sensitive to temperature. The sensitivity of the coarse sand to each atmospheric parameter is more than that for fine sand and clay soil. Different trends of sensitivity with time were observed at different depths. The fine sand and coarse sand soil exhibit decreasing sensitivities to temperature at the surface and an increasing trend in time at depths below 5 cm (2 in). Whereas the clay soil's sensitivity to temperature increased with time at the top 5 cm layer only and remained insensitive at the depth below that. All three soil types showed increasing sensitivity to wind speed with time.

The sensitivity graphs provide valuable insight into the variations in MC in the field with changes in atmospheric parameters.

3. Chapter 3: Test Pit Modeling

This chapter includes a summary of the construction and instrumentation of three large test pits at the Federal Highway Administration's Turner Fair Highway Research Center (TFHRC). Complete details of the construction, volumetric water sensors instrumentation and calibration, weather conditions, and collected data are provided in Khosravifar (2015).

The objective of this chapter is to evaluate and compare the VWC history measured in the field by Khosravifar (2015) to the values predicted by SVFlux.

3.1. Test pit construction

The test pit dimensions were approximately 4.6 $m\times$ 4.6 $m\times$ 2.4 m (15 $ft\times$15 $ft\times$ 8 ft) each (Figure 3-1). Ruggedized Decagon GS-1 sensors were used to measure the VWC of the soils via the dielectric constant. The sensors for this study were embedded at the final layer of pit 1 and pit 3 at depths of about 8.5 cm (3.35 in) and 5.4 cm (2.12 in) respectively. They could not be placed closer to the surface since a sheep foot vibratory roller compactor was used for compaction of each layer and there was a risk of damaging or breaking the sensors and wiring under the compactor's pressure and vibration.

The VWC data were then collected from the compacted base material in pit 3 (designated as M4) for nearly 5 days and from the subgrade material in pit 1 (sensor M5) for about 3 days.

Figure 3-1. Final level of compacted test pits, VA21a base material (left picture) and ALF subgrade (right picture).

3.2. Soil characterization

The base material compacted as the final layer of pit 3 was a well graded aggregate base routinely used in state of Virginia and referred to as VA21a stone. The non-cohesive silty sand soil compacted in pit 1 was the local subgrade used at the TFHRC accelerated loading facility (ALF).

Table 3-1 presents the Unified soil classification and Atterberg Limits obtained according to AASHTO T-89 and T-90 for the soils of this study.

Table 3-1. Selected properties of the soils used in test pit construction (from Khosravifar, 2015).

Soil Type	Soil Classification	D30	D10	D60	Cc	Cu	Atterberg Limits			Specific Gravity
							LL	PL	PI	
ALF	SM	1.7	0.3	6.6	1.7	25.1	-	-	-	2.68
VA21a	GW	-	-	0.2	-	-	31	27	5	2.68

Figure 3-2 and Figure 3-3 show the gradation and SWCC of the materials. The gradation curves were obtained according to AASHTO T-27 for VA21a and according to AASHTO T-11 and T-27 for the ALF (Khosravifar, 2015). The SWCCs were estimated using four-parameter equation proposed by Fredlund and Xing (1994).

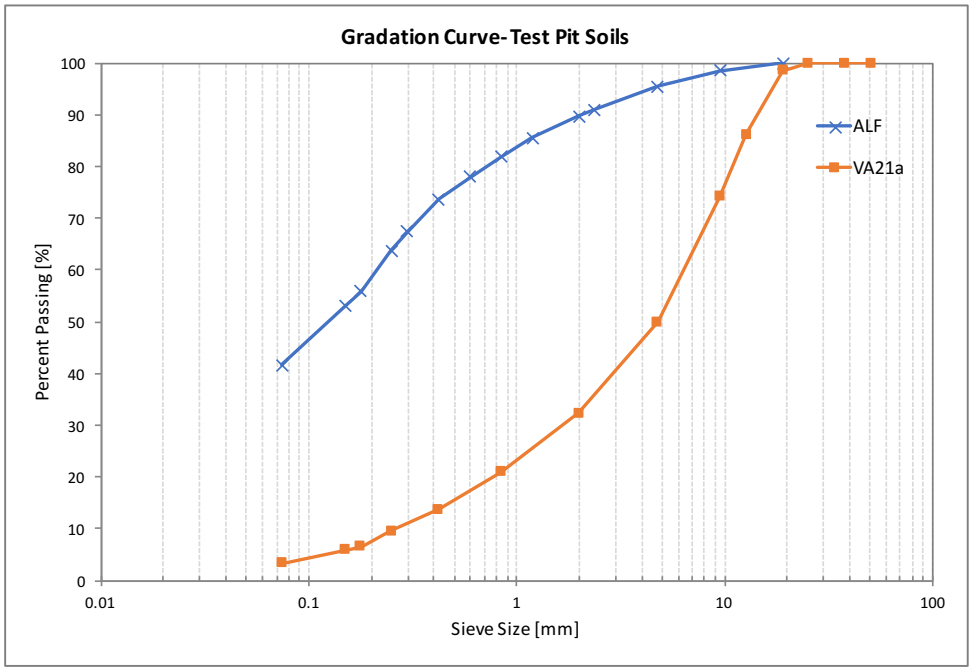

Figure 3-2. Gradation curve for the soils used in test pit construction (from Khosravifar, 2015).

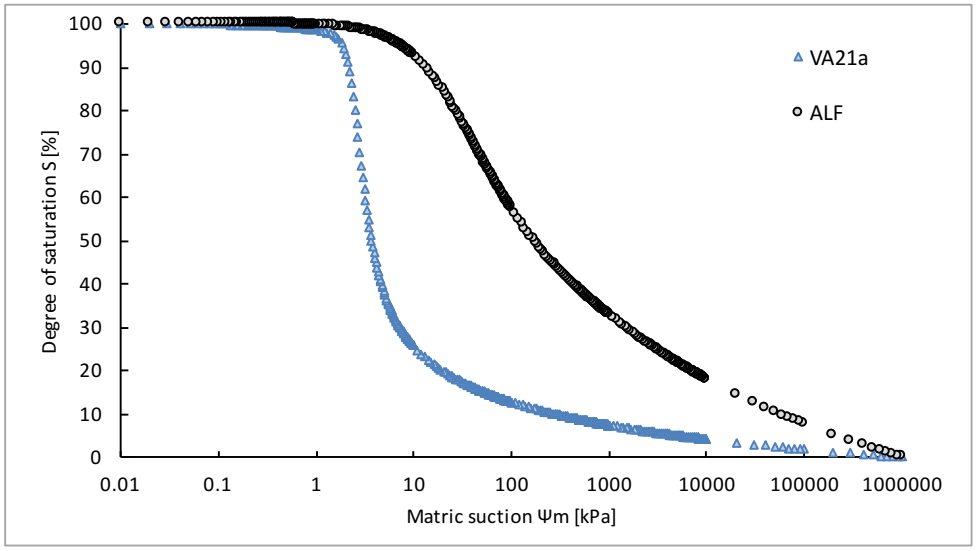

Figure 3-3. Soil water characteristic curve for the soils used in test pit construction (from Khosravifar, 2015).

3.3. SVFlux modeling

The ALF subgrade in the pit 1 is simulated by a 1D soil column 50 cm (20 in) tall with a Climate BC at the top. Since the test pit 1 was already half filled with uncompacted uniform crushed stone covered with a layer of geotextile (Figure 3-4), the bottom boundary condition was selected as Flux BC.

The VA21a base layer in pit 3 was 10.7 cm in depth (4.2 in) compacted on top of a compacted high plasticity clay (HPC). Since the hydraulic conductivity of the HPC is very low (10^{-10} to 10^{-6} cm/s), the soil column boundary condition is set to zero flux at the bottom. The Climate BC was applied to the surface.

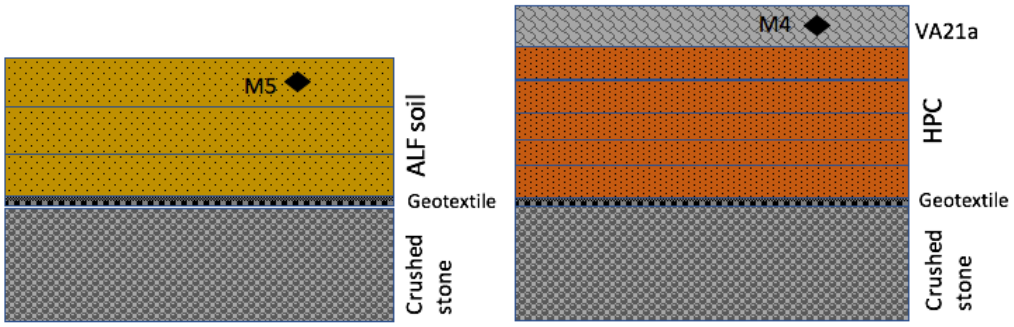

Figure 3-4. Test pits soil layers' profile and embedded VWC sensor location, pit 1 (left) and pit 3 (right picture).

The climate inputs for SVFlux were obtained from the weather conditions captured during the construction and testing of the pits. Wind speed, air temperature, humidity, and potential evaporation rate were recorded using the Kestrel weather tracker (data available at Khosravifar, 2015). The test pits were fully covered by a tent during the construction and testing. Therefore, the sunshine ratio is considered zero for the net radiation calculation by SVFlux.

Saturated hydraulic conductivity was roughly estimated as 17.28 m/day for the VA21a granular base and 1 m/day for the ALF subgrade (Das, 2014, Table 6.1). Unsaturated hydraulic conductivity was estimated by the modified Campbell method.

The predicted VWC values were output at the same locations as the embedded sensors—i.e., 8.5 cm (3.35 in) depth for the 1 and 5.4 cm (2.12 in) depth for pit 3.

3.4. Results

Figure 3-5 compares the measured VWC from the embedded sensors in the VA21a aggregate (M4) and the SVFlux predicted values (series 1) versus time. The VWC dropped from 8.5% to 7.41% at the 5.4 depth after about five days. The SVFlux results over predict the VWC by 0.2 to 0.4 percentage points (approximately 5%).

Figure 3-6 compares the measured VWC in the ALF subgrade (M5) and the SVFlux predicted values (series 1) versus time. The VWC measured by the GS-1 sensor dropped from 16.25% to 14% after three days while the simulated VWC dropped only to 15.13%. The SVFlux results are generally over predicting the measured VWC and the discrepancies increase over time. The predicted water content is 1.1 percentage points (approximately 8%) more than the measured values at the end of the third day.

3.5. Conclusions

The VWC history measured by Decagon's GS-1 sensors for two soil types were compared to the VWC values predicted by the SVFlux software. SVFlux proved to be a useful tool for predicting the drying in the soils overtime. The simulated results generally over predicted the drying for both soils. This most likely is due to the estimation of hydraulic conductivity for the soil materials. The uncoupled simulation of evaporation may also be a contributing factor.

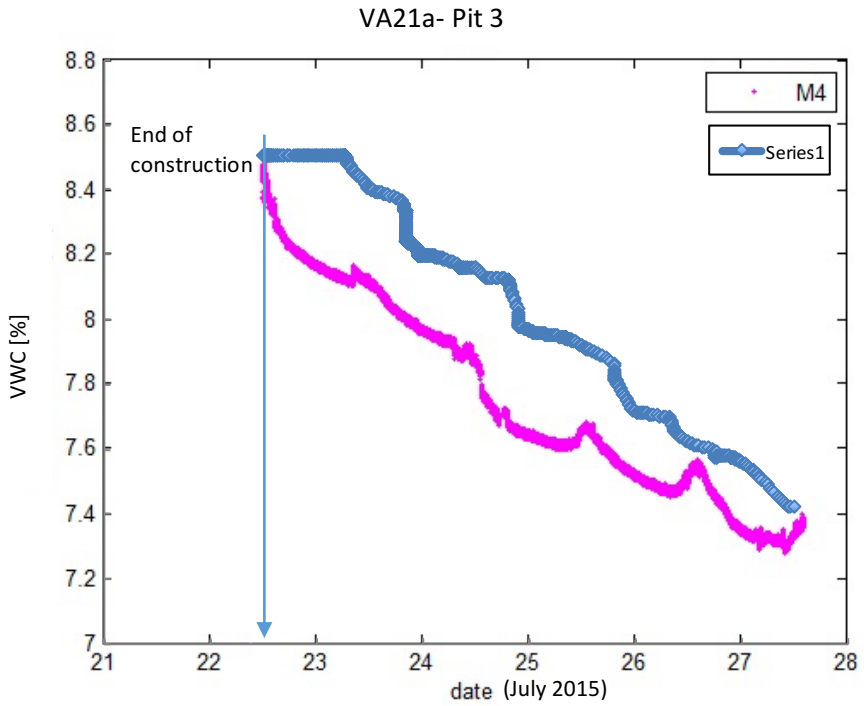

Figure 3-5. VWC measurement by GS-1 embedded sensors (M4) comparing to VWC simulation by SVFlux (Series 1) for VA21a soil.

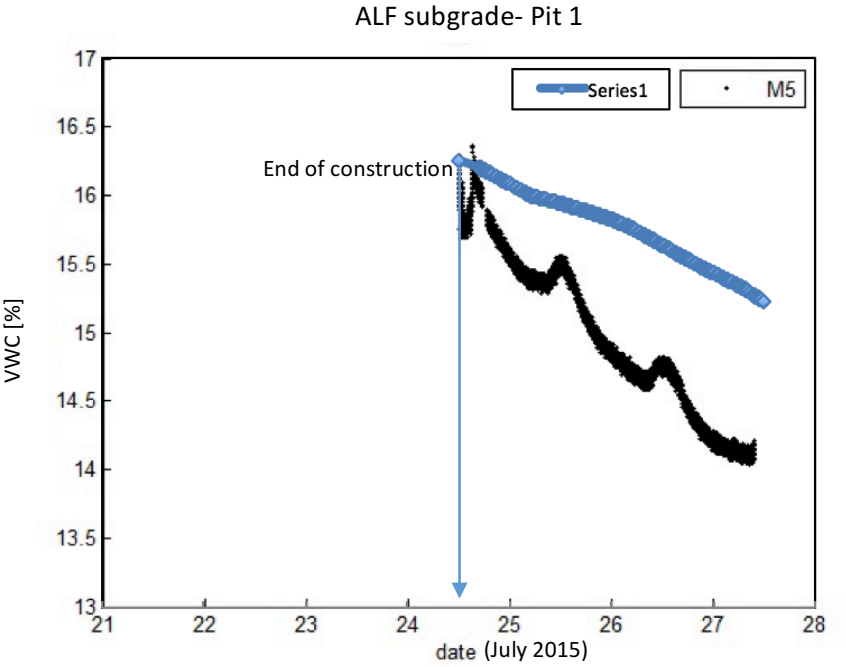

Figure 3-6. VWC measurement by GS-1 embedded sensors (M5) comparing to VWC simulation by SVFlux (Series 1) for ALF soil.

4. Chapter 4: Field Evaluations

This chapter presents the results of a field study to investigate the effect of post compaction drying on lightweight deflectometer (LWD) surface moduli. Four projects were selected to perform LWD and MC testing for up to several hours after compaction.

4.1. Selected LWD devices

The LWD is a portable device that measures the in-situ modulus of the soil under an impact loading. There are different types of LWDs with different configurations commercially available. Generally, the device consists of a mass of certain weight that freely slides on a guiding rod and is dropped onto buffers attached to the loading plate. The loading plate should be in full contact with the compacted soil and can be changed to different sizes, depending on the soil type and application. Then the deflection on the plate (solid plate type) or on the ground surface (annulus plate type) is measured using an accelerometer or a geophone.

The modulus is calculated using the Boussinesq equation from theory of elasticity:

Equation 4-1

$$E = \frac{2k_s(1-v^2)}{Ar_0}$$

in which k_s is the maximum applied load to maximum deflection ratio, A is the stress distribution factor (A=4 for cohesive soils, 3π/4 for granular material, and π for mixed soil), v is Poisson's ratio, and r_0 is the plate radius.

Three types of LWD devices were employed to span the typical differences among commercial devices: a Zorn ZGF 3.0, a Dynatest 3031, and an Olson LWD-01. Table 4-1 presents the characteristics and configurations of each LWD used in this

study. LWD testing was performed on 10 to 15 different location at 10 ft intervals in accordance with ASTM E 2583 for devices with a load cell and ASTM E 2835 for devices without a load cell (Figure 4-1, A). A stress distribution factor of π, Poisson's ratio of 0.35, and plate size of 300 mm (12 in) were used for all projects in this study.

Table 4-1. LWD devices characteristics.

LWD	Falling weight [kg]	Max height [cm]	Load cell	Deflection sensor		Loading plate		Buffer type
				type	range [mm]	type	diameter [mm]	
Zorn ZFG 3.0	10	72.4	No	Accelerometer	0.2-30 (±0.02)	solid	100, 150, 200, 300	Spring
Dynatest 3031	5, 10, 15, 20	83.8	Yes	Geophone +2 external	0-2.2 (±0.002)	annulus w/ plugin option	100, 150, 200, 300	Flat rubber (adjustable)
Olson 01	10	60	Yes	Geophone +2 external	N/A	solid	100, 150, 200, 300	Spring

A)  B) 

Figure 4-1. (A) LWD testing at a location in the field using Olson, Zorn, and Dynatest LWD (from left to right). (B) Fluke Infrared Thermometer (left) and Kestrel 4300 Construction Weather Tracker (right).

4.2. Soil characterization

Table 4-2 presents the location and soil classification for four soil types. Two of the soils were subgrades and two were granular base materials. Table 4-3 includes routine

soil properties and Figure 4-2 to Figure 4-5 show the gradation curve for the selected material. The gradations were obtained according to AASHTO T-27, T-11, and T-27.

The weather conditions for wind speed, air temperature, humidity and evaporation rate were recorded using the Kestrel weather tracker during testing. Additionally, the soil surface temperature was measured using a Fluke infrared thermometer at various random locations (Figure 4-1B). The results are presented in Table 4-4. Further project details and description are provided in the following sections.

Table 4-2. Project location and soil classification.

Location	Soil Type	AASHTO Classification	Unified Classification	
Maryland	MD 5 subgrade	A-1-a	SP	Poorly graded sand with gravel
New York	Embankment (local subgrade)	A-3	SP	Poorly graded sand
Missouri	MO Base	A-1-a	GW	Well graded gravel with sand
Florida	FL Base	A-1-b	SP	Poorly graded gravel with sand

Table 4-3. Selected soil properties.

Location and Soil Type	D30	D10	D60	Cc	Cu	Atterberg Limits			Specific Gravity
						LL	PL	PI	
MD 5, subgrade	0.79	0.40	9.42	0.16	23.54	-	-	non-plastic	2.69
New York, embankment	0.24	0.14	0.36	1.19	2.56	-	-	non-plastic	2.68
Missouri, GAB	2.09	0.34	8.15	1.59	24.17	-	-	non-plastic	2.62
Florida, Base	0.45	0.23	2.49	0.34	10.66	-	-	non-plastic	2.46

Table 4-4. Project weather condition and soil surface temperature.

Project name	Soil temperature, C	Wind speed Km/h	Air temperature, C	Humidity, %	Evaporation Rate
MD 5	31	4-9	25	53.3%	0.61-0.77
NY	28	4-9	29.1	61.0%	0.25-0.53
MO	25	0	25	54.0%	0.13
FL	20	3-10	24.7	60.0%	0.05-0.08

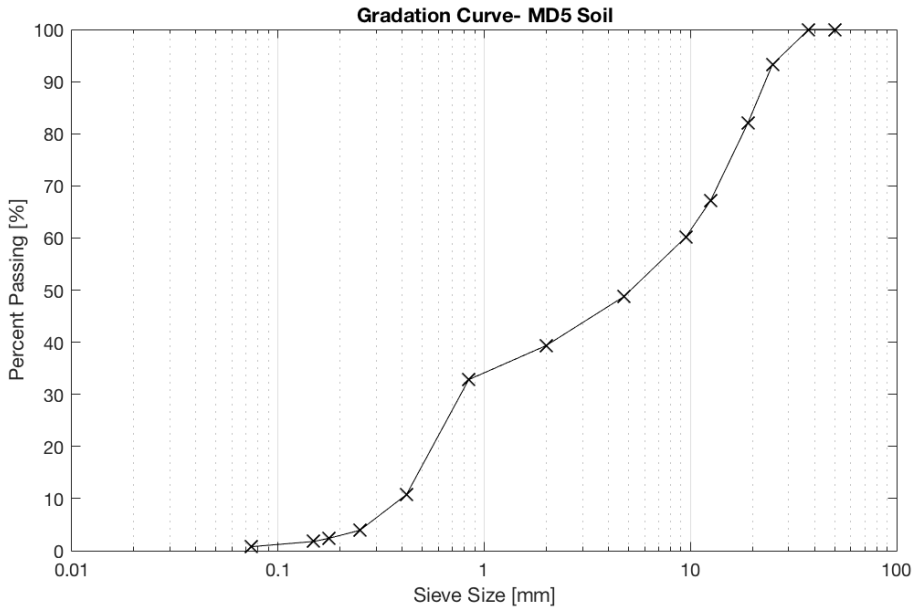

Figure 4-2. Gradation curve for the MD 5 soil.

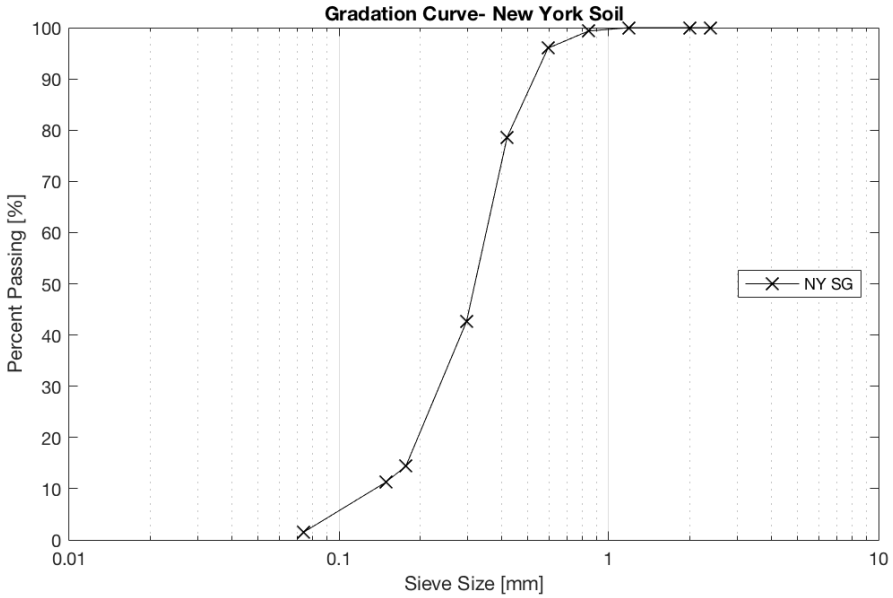

Figure 4-3. Gradation curve for the NY soil.

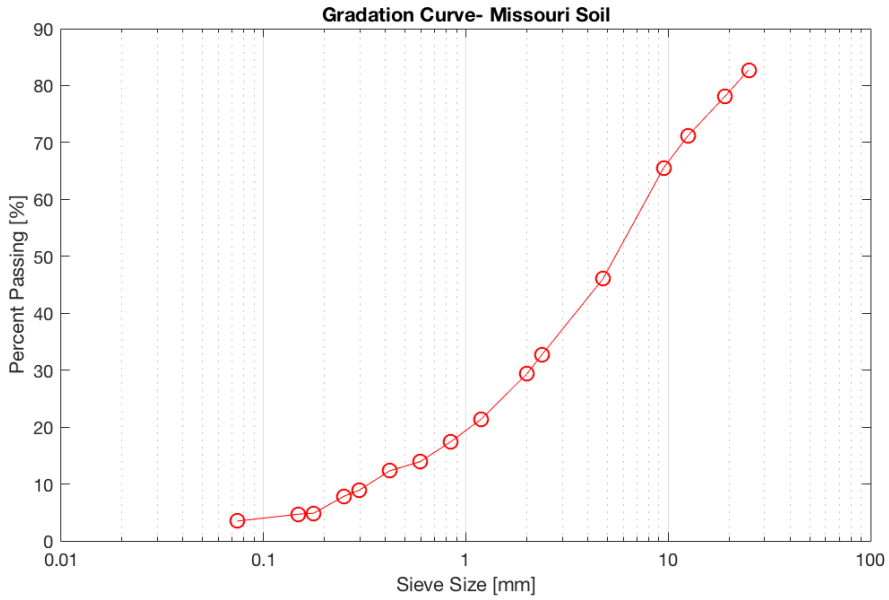

Figure 4-4. Gradation curve for the MO soil.

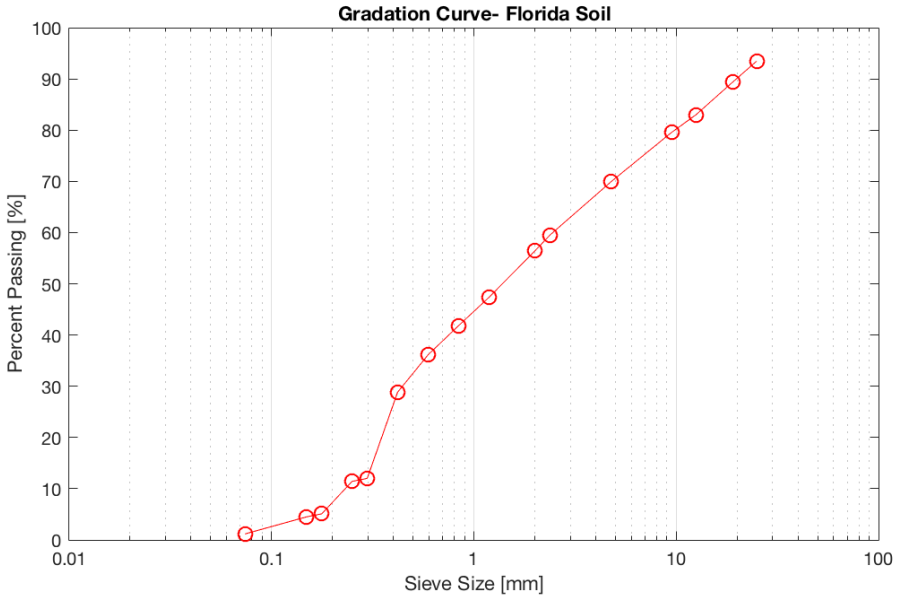

Figure 4-5. Gradation curve for the FL soil.

4.3. Results for MD 5 road construction project

MD 5 embankment construction and subgrade compaction on the embankment was located from Auth road to South of I-495/I-95. The poorly graded sand with gravel material was placed over the dried embankment with a slope of about 3%. Testing was carried out in three rounds: immediately after placement and compaction and then 2 and 3 hours later.

Soil samples were extracted from a depth of 3 to 5 inches below the surface of the compacted layer at all test spots and sealed for moisture content measurement via oven drying in the lab per AASHTO T 265. Figure 4-6 presents the MC in the field at each location for each round of testing.

Figure 4-7 shows the measured average MC versus time superimposed by the average field modulus after compaction for the three LWDs. Error bars depict the standard deviation. The average MC loss after 3 hours is about 1.5 percentage points. The Zorn LWD modulus increased by 5% on average and the Dynatest modulus increased by about 20% on average after 3 hours. The Olson LWD paradoxically showed a decrease of about 12% after drying.

To assess the increase in modulus after compaction, a two-sample t-test is performed using MS Excel, assuming unequal variances. For this purpose, the null hypothesis (H0) states that the difference between the means is zero, i.e. the average modulus of compacted material did not change significantly due to drying. The alternative hypothesis (Ha) is that the difference between the means is more or less than zero. The significance level (α) is defined as the probability of making the wrong decision when the null hypothesis is true. A significance level of 5% is assumed. In a two-tail t-test, when t-Stat is less than -t Critical, or t-Stat is more than t Critical, the null hypothesis is rejected.

Table 4-5, Table 4-6, and Table 4-7 present the results of the t-test for Zorn, Dynatest, and Olson LWDs respectively. Since the t-Stat is within the range of -t Critical to t Critical (two-tail), the observed difference between the mean moduli of first and third round of testing after 3 hours is not significant.

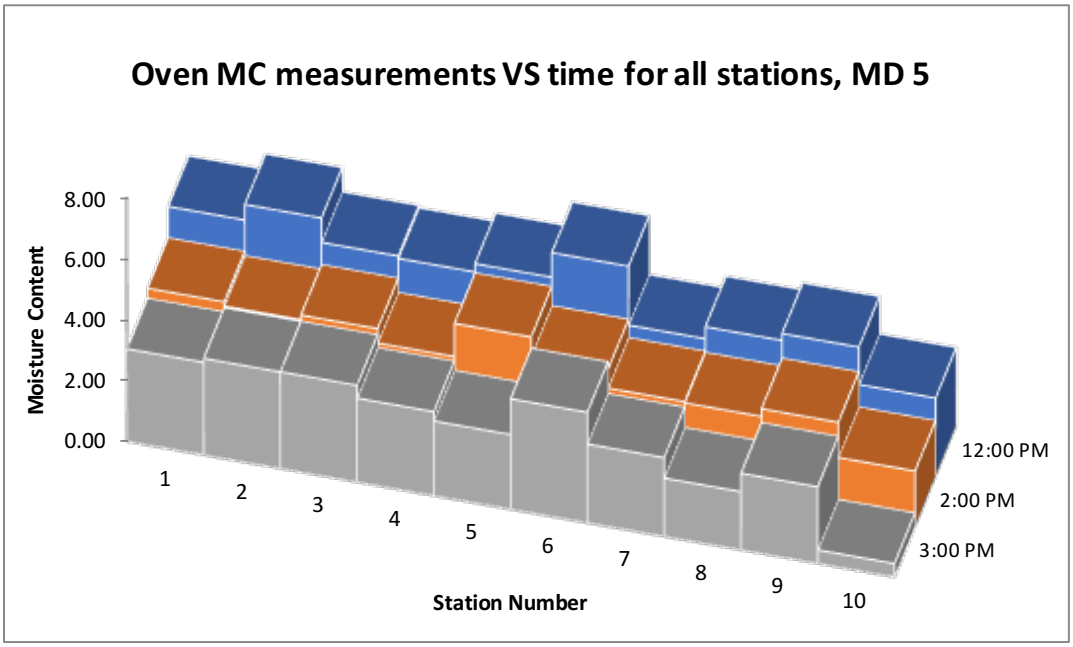

Figure 4-6. MC samples measured by oven drying method for all stations few hours after compaction for MD 5 project.

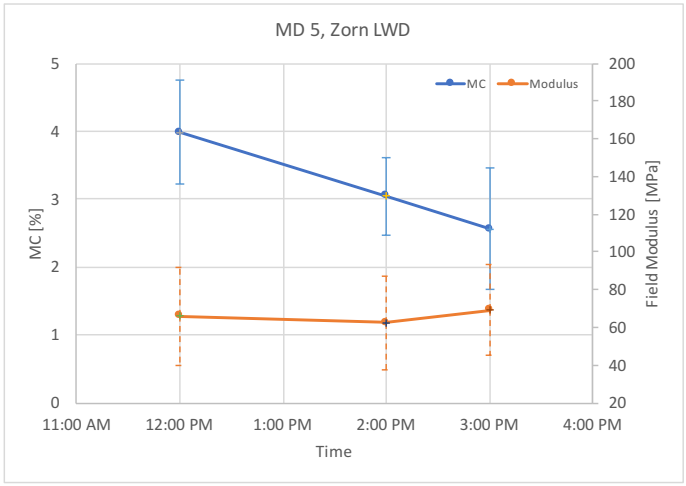

A)

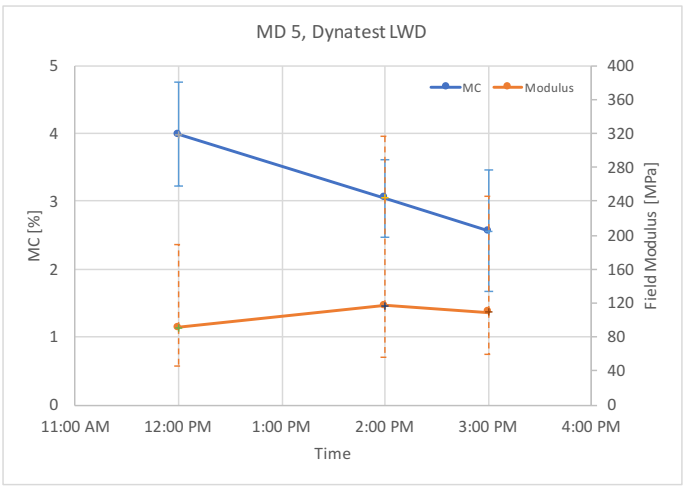

B)

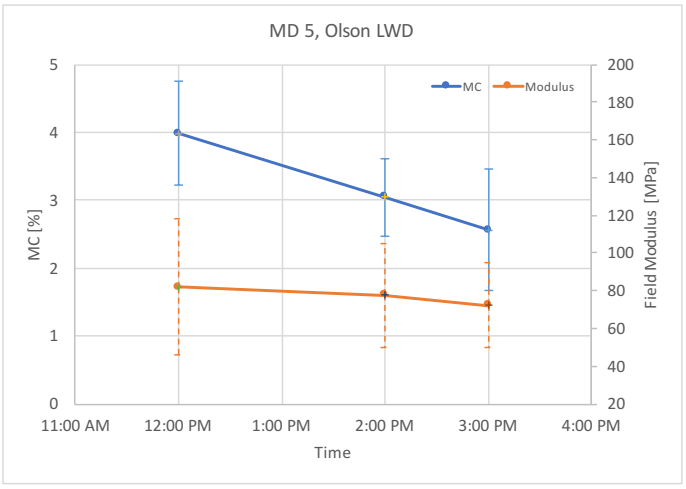

C)

Figure 4-7. Measured average MC in the field versus time superimposed by the average field modulus versus time after compaction for MD 5 project. Modulus measured by (A) Zorn LWD, (B) Dynatest LWD, and (C) Olson LWD.

Table 4-5. t-Test results for Zorn LWD modulus values (E1: modulus values at 12:00 PM, and E3: modulus values at 3:00 PM), MD 5 construction

	E1	*E3*
Mean	65.95	69.26
Variance	665.68	570.69
Observations	10	10
Hypothesized Mean Difference	0	
df	18	
t Stat	-0.2975	
P(T<=t) one-tail	0.3847	
t Critical one-tail	1.7341	
P(T<=t) two-tail	0.7695	
t Critical two-tail	2.1009	

Table 4-6. t-Test results for Dynatest LWD modulus, MD 5 construction

	E1	*E3*
Mean	90.98	108.94
Variance	1869.84	3295.02
Observations	9	9
Hypothesized Mean Difference	0	
df	15	
t Stat	-0.7495	
P(T<=t) one-tail	0.2326	
t Critical one-tail	1.7531	
P(T<=t) two-tail	0.4652	
t Critical two-tail	2.1314	

Table 4-7. t-Test results for Olson LWD modulus values, MD 5 construction

	E1	*E3*
Mean	82.10	72.24
Variance	1308.94	501.55
Observations	10	10
Hypothesized Mean Difference	0	
df	15	
t Stat	0.7330	
P(T<=t) one-tail	0.2374	
t Critical one-tail	1.7531	
P(T<=t) two-tail	0.4748	
t Critical two-tail	2.1314	

4.4. Results for New York embankment construction

The Luther Forest Boulevard extension project located in Albany NY used local uniform sand for an embankment compacted in layers of 8 to 12 in thickness. Testing was carried out on two lifts for two rounds using the Zorn LWD and two rounds on the second lift only for the Olson LWD. A Dynatest LWD was not available for this field trip.

Oven moisture content results are presented in Figure 4-8 for each lift (L1 and L2) at one hour intervals. Figure 4-9 exhibits the measured average MC versus time superimposed by the average field modulus after compaction for the two LWDs. Error bars depict the standard deviation.

The average MC losses after one hours were 0.07 percentage points for the lift 1 and 0.11 percentage points for the lift 2. The average Zorn LWD modulus is increased by 7.6% for the lift 1 and 2% for the lift 2 after one hour of drying. The average Olson modulus increased only by 0.3% after one hour of drying.

Similar to section 4.3, a two-sample t-test is used to evaluate the stiffness gain due to drying in the field after an hour. Similar H0, Ha, and significance level is assumed.

Table 4-8 presents the results of the t-test for Zorn LWD for the two compacted lifts. Table 4-9 present the t-test results for Olson LWD modulus values for the second lift construction. As observed, the t-Stat is within the range of -t Critical to t Critical two-tail for the two LWDs. Therefore, the difference between the mean moduli tested right after compaction (E1), and tested an hour later (E2) is not significant.

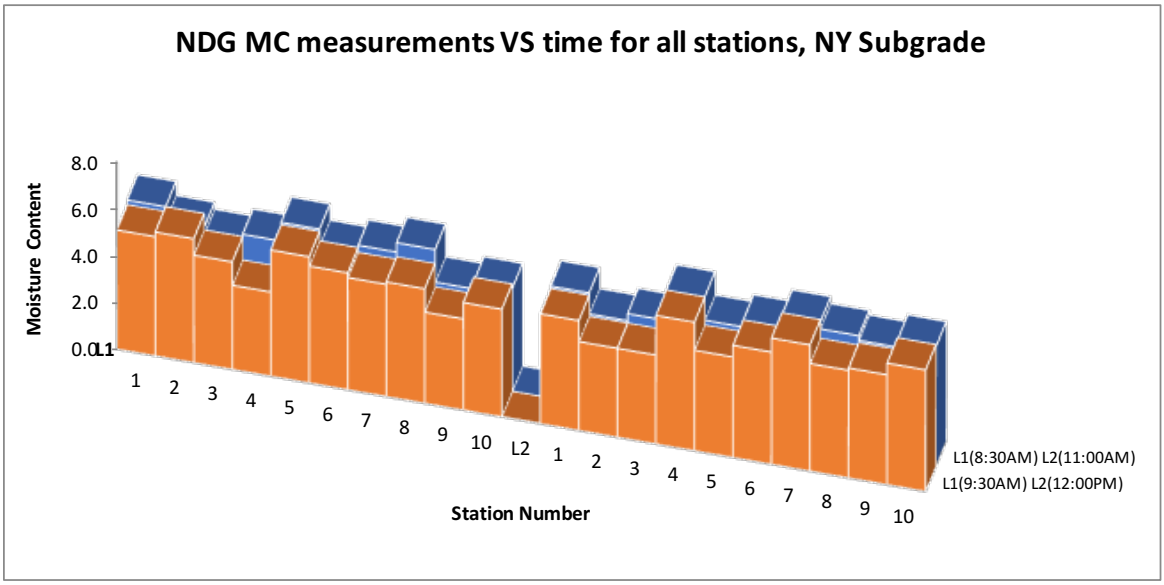

Figure 4-8. MC samples measured by oven drying method for all stations immediately and an hour after compaction of first lift (L1) and second lift (L2) for NY project.

A)

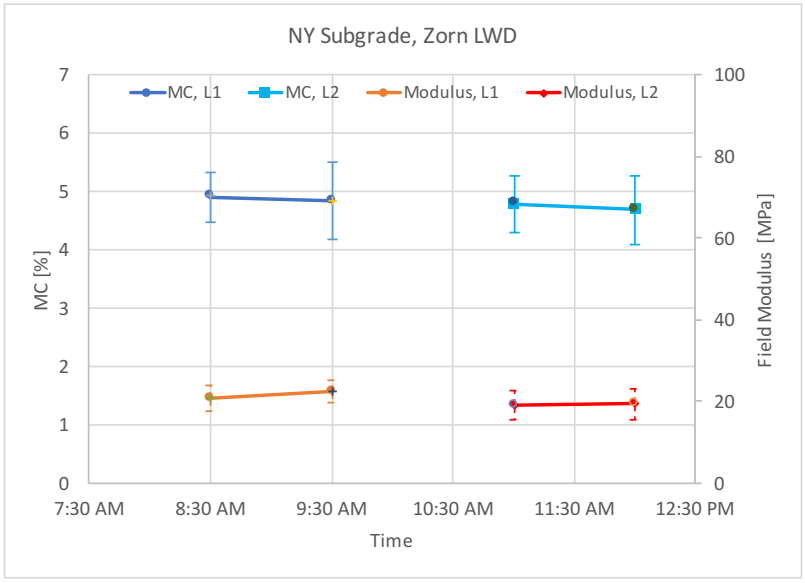

B)

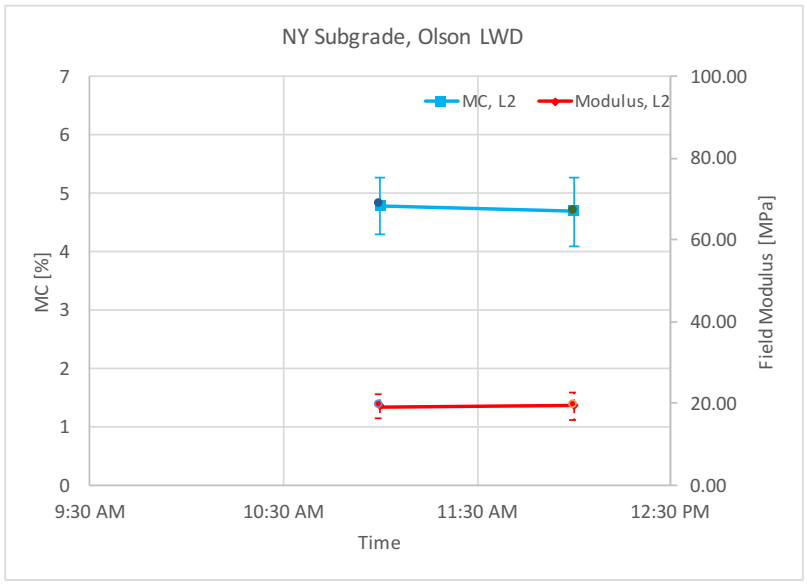

Figure 4-9. Measured average MC in the field versus time superimposed by the average field modulus versus time after compaction for NY project. Modulus measured by (A) Zorn LWD, and (B) Olson LWD (L1: lift 1, and L2: lift 2)

Table 4-8. t-Test results for Zorn LWD modulus values, NY subgrade compaction

Lift 1	*E1*	*E2*
Mean	20.75	22.34
Variance	10.14	7.58
Observations	6	6
Hypothesized Mean Difference	0	
df	10	
t Stat	-0.9219	
P(T<=t) one-tail	0.1891	
t Critical one-tail	1.8125	
P(T<=t) two-tail	0.3783	
t Critical two-tail	2.2281	
Lift 2	*E1*	*E2*
Mean	19.10	19.50
Variance	12.93	14.26
Observations	10	10
Hypothesized Mean Difference	0	
df	18	
t Stat	-0.2442	
P(T<=t) one-tail	0.4049	
t Critical one-tail	1.7341	
P(T<=t) two-tail	0.8098	
t Critical two-tail	2.1009	

Table 4-9. t-Test results for Olson LWD modulus values, NY subgrade compaction

Lift 2	*E1*	*E2*
Mean	19.30	19.37
Variance	8.92	12.37
Observations	10	10
Hypothesized Mean Difference	0	
df	18	
t Stat	-0.0457	
P(T<=t) one-tail	0.4820	
t Critical one-tail	1.7341	
P(T<=t) two-tail	0.9641	
t Critical two-tail	2.1009	

4.5. Results for Missouri lane widening project

The MO project was lane widening and shoulder compaction for I-64. The concrete shoulder on the I-64 lane was removed and the subgrade below the concrete was compacted with 1 to 2 passes of a roller compactor. Then a 4 inch layer of crushed limestone (base) was placed on top of the subgrade. Testing using all three LWDs was carried out in two rounds: right after placement and compaction and then one hour later.

Oven-dried moisture content results are presented in Figure 4-10 for each round. Figure 4-11 illustrates the measured average MC versus time superimposed by the average field modulus after compaction. Error bars depict the standard deviation.

Even though the average MC loss after one hours was only 0.14 percentage points, the Zorn LWD modulus increased by 18.5%, the Dynatest modulus increased by 20.7%, and the Olson modulus increased by 18.5% on average.

A two-sample t-test is used to evaluate the significance of the modulus gain due to drying in the field after an hour. Similar H0, Ha, and significance level is assumed.

Table 4-10, Table 4-11, and Table 4-12 present the results of the t-test for Zorn, Dynatest, and Olson LWDs respectively. Since the t-Stat is within the range of -t Critical to t Critical two-tail, the average moduli tested right after compaction (E1) is not significantly different than the modulus values tested after an hour (E2).

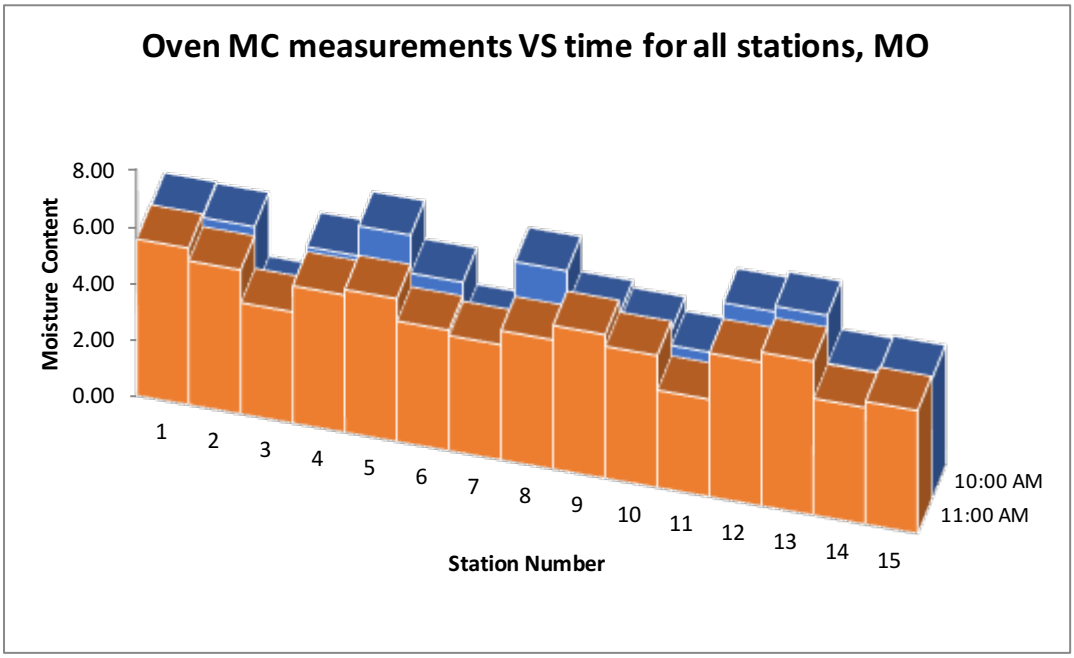

Figure 4-10. MC samples measured by oven drying method for all stations immediately and an hour after compaction for MO project.

A)

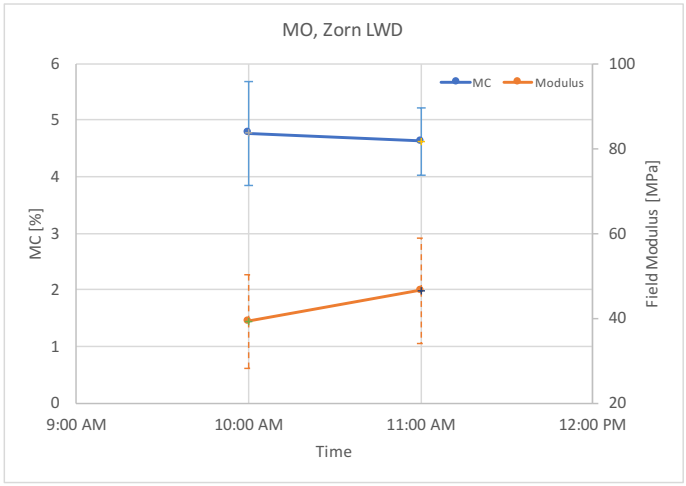

B)

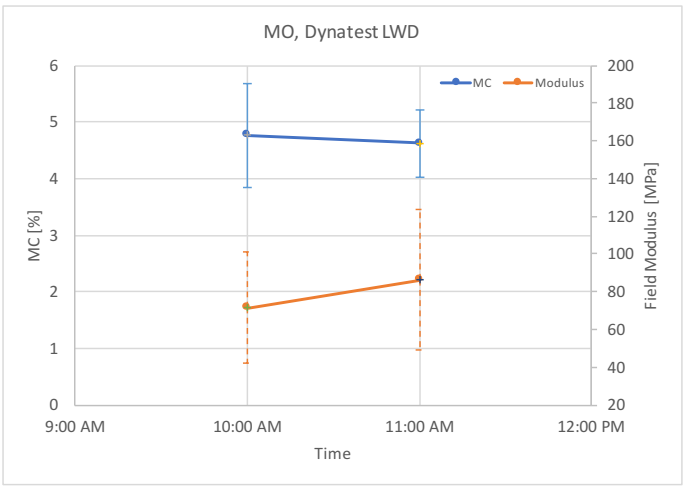

C)

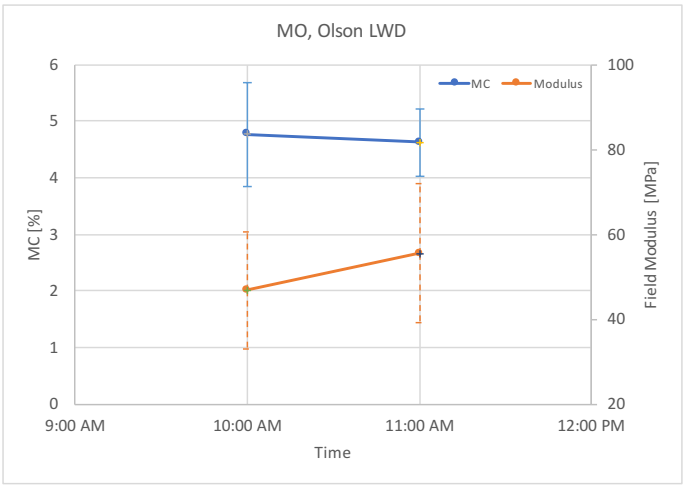

Figure 4-11. Measured average MC in the field versus time superimposed by the average field modulus versus time after compaction for MO project. Modulus measured by (A) Zorn LWD, (B) Dynatest LWD, and (C) Olson LWD.

Table 4-10. t-Test results for Zorn LWD modulus values, MO base

	E1	*E2*
Mean	39.21	46.45
Variance	121.87	156.45
Observations	15	15
Hypothesized Mean Difference	0	
df	28	
t Stat	-1.6821	
P(T<=t) one-tail	0.0518	
t Critical one-tail	1.7011	
P(T<=t) two-tail	0.1037	
t Critical two-tail	2.0484	

Table 4-11. t-Test results for Dynatest LWD modulus values, MO base

	E1	*E2*
Mean	71.45	86.25
Variance	878.11	1374.96
Observations	15	15
Hypothesized Mean Difference	0	
df	27	
t Stat	-1.2076	
P(T<=t) one-tail	0.1188	
t Critical one-tail	1.7033	
P(T<=t) two-tail	0.2377	
t Critical two-tail	2.0518	

Table 4-12. t-Test results for Olson LWD modulus values, MO base

	E1	*E2*
Mean	46.83	55.49
Variance	191.17	265.19
Observations	15	15
Hypothesized Mean Difference	0	
df	27	
t Stat	-1.5701	
P(T<=t) one-tail	0.0640	
t Critical one-tail	1.7033	
P(T<=t) two-tail	0.1280	
t Critical two-tail	2.0518	

4.6. Results for Florida road construction project

The SR 23 road construction in South Jacksonville, FL was an extension from SR 21 (Blanding Blvd.) to the Duval county line. The subgrade was compacted a week in advance. Then the local limerock base was placed and compacted to a thickness of 6 to 8 in on top of the dried subgrade.

LWD testing was carried out for two rounds at a one hour interval using the Zorn LWD and Dynatest LWDs. The Olson LWD was not available for this field trip.

Oven dried moisture content results are presented in Figure 4-12. Figure 4-13 shows the measured average MC versus time superimposed with the average field modulus after compaction for the two LWDs. Error bars depict the standard deviation.

The average MC loss after one hours is 0.07 percentage points for this material. The Zorn LWD modulus increased by 10.3% and Dynatest LWD modulus increased about 24% on average as a result of drying.

The results of the two-sample t-test is presented in Table 4-13 and Table 4-14 for Zorn and Dynatest LWDs respectively. Similar H0, Ha, and significance level is assumed.

The t-Stat is within the range of -t Critical to t Critical two-tail for Zorn LWD modulus value, therefore the average increase in modulus is insignificant after an hour. However, the Dynatest LWD t-Stat is lower than the -t Critical for the FL limerock base, meaning that the null hypothesis rejected. The observed difference between the modulus means is convincing enough to state that the Dynatest modulus values differed significantly after one hour.

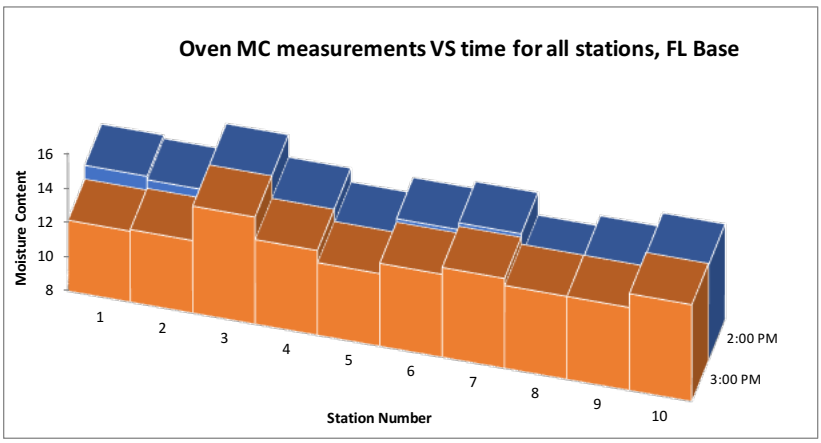

Figure 4-12. MC samples measured by oven drying method for all stations immediately and an hour after compaction for FL project.

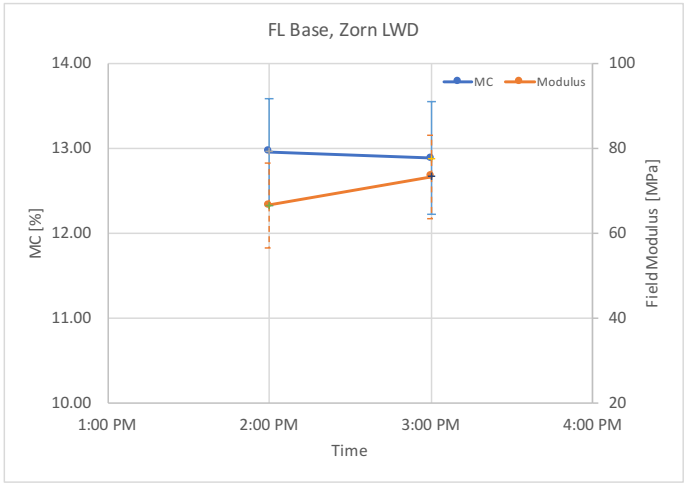

A)

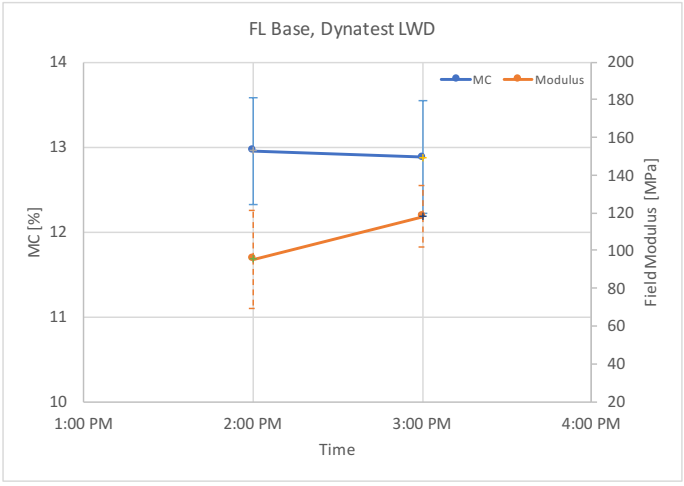

B)

Figure 4-13. Measured average MC in the field versus time superimposed by the average field modulus versus time after compaction for FL project. Modulus measured by (A) Zorn LWD, and (B) Dynatest LWD.

Table 4-13. t-Test results for Zorn LWD modulus values, FL base

	E1	*E2*
Mean	66.41	73.26
Variance	103.13	97.18
Observations	10	10
Hypothesized Mean Difference	0	
df	18	
t Stat	-1.5307	
P(T<=t) one-tail	0.0716	
t Critical one-tail	1.7341	
P(T<=t) two-tail	0.1432	
t Critical two-tail	2.1009	

Table 4-14. t-Test results for Dynatest LWD modulus values, FL base

	E1	*E2*
Mean	95.33	118.18
Variance	684.65	272.75
Observations	10	10
Hypothesized Mean Difference	0	
df	15	
t Stat	-2.3355	
P(T<=t) one-tail	0.0169	
t Critical one-tail	1.7531	
P(T<=t) two-tail	0.0338	
t Critical two-tail	2.1314	

4.7. Conclusions

The variation of modulus with time was compared a few hours after compaction for two subgrades and two base soil types. Overall, the Dynatest LWD exhibited more stiffness gain due to drying after compaction, since it measures the deflection directly on top of the soil, and the drying occurring on the surface would easily affect the deflection and modulus data. The Zorn and Olson LWD show a stiffness gain of less than 10% for subgrade soils due to drying. However, for the crushed limestone and limerock base materials, drying of even less than 1 percentage point increased the measured field moduli by up to 20%. A two-sample t-Test was performed to evaluate the significance of modulus gain due to drying. For all materials and LWD types, the observed difference between the sample modulus means is not convincing enough to state that the average modulus increased significantly due to drying a few hours after compaction (except for Dynatest modulus values for FL Limerock base compaction). Generally, the modulus of granular base materials is more sensitive to drying in the field.

5. Chapter 5: Conclusions

A literature review of past studies of drying in soils is presented in the first chapter. Most of the past studies focused on the drying process in earthen material, drying effects on hydraulic properties and drainage, or the effect of atmospheric parameters on the SWCC. There is a lack of information on the effect of MC on structural adequacy of compacted soil under unsaturated conditions.

The physical process of evaporation from the soil is briefly described in chapter 2 along with modeling steps required in SVFlux software. Then moisture loss profiles were predicted for three different soil types from Yanful and Choo (1997) for a 24-hour time span. SVFlux proved to be useful as a tool to predict the MC and drying depth in soils after placement.

To investigate the sensitivity of the soils to atmospheric factors such as temperature, wind speed, and relative humidity, the three soil types (fine sand, coarse sand, and clay soil) were analyzed for changes in one atmospheric variable while keeping all other parameters constant. Temperature was found to be the most important parameter affecting the moisture loss in the soils. The coarse sand demonstrated the most sensitivity to the atmospheric parameters, whereas the clay soil had the lowest sensitivity, especially at the surface. The sensitivity graphs provide valuable insights into the effects of drying under various weather conditions.

To compare the actual MC with the simulated results for validation purposes, the VWC histories measured using Decagon GS-1 sensors were compared to the predicted VWC from SVFlux simulations for two soil types. The simulated results slightly over predicted the MC. The SVFlux simulation package can be a useful tool for transient MC prediction. However, the coupled heat and water flow simulation should be performed with accurate hydraulic conductivity values for best results.

Finally, to investigate the effect of drying on the soil stiffness in a practical field situation, LWD modulus values were captured for up to several hours after compaction at four project sites: two with poorly graded sand subgrade and two with crushed limestone/limerock gravel base material (one well graded and one poorly graded).

The Dynatest LWD exhibited more stiffness gain due to drying after compaction, for the geophone is in direct contact with the soil surface. The Zorn and Olson LWDs reported stiffness gains of less than 10% for subgrade soils due to drying. The base materials showed a larger gain in modulus during the first few hours after compaction. Large coefficients of variation were observed for both the MC and modulus data in the field, which complicates determining consistent trends in average modulus increase due to drying. A t-Test should be employed to assess the significance of modulus gain due to drying in the field.

References

AASHTO, T. 11-05, (2009). Standard Method of Test for Materials Finer Than 75-micrometer (No. 200) Sieve in Mineral Aggregates by Washing*, American Association of State Highway and Transportation Officials, Washington, DC.*

AASHTO, T. 180-10, (2014). Standard Method of Test for Moisture-Density Relations of Soils Using a 4.54-kg (10-lb) Rammer and a 457-mm (18-in.) Drop*, American Association of State Highway and Transportation Officials, Washington, DC.*

AASHTO, T. 265-15, (2015). Standard Method of Test for Laboratory Determination of Moisture Content of Soils*, American Association of State Highway and Transportation Officials, Washington, DC.*

AASHTO, T. 27-11, (2011). Standard Method of Test for Sieve Analysis of Fine and Coarse Aggregates*, American Association of State Highway and Transportation Officials, Washington, DC.*

AASHTO, T. 89-13, (2013). Standard Method of Test for Determining the Liquid Limit of Soils*, American Association of State Highway and Transportation Officials, Washington, DC.*

AASHTO, T. 90-00, (2008). Standard Method of Test for Determining the Plastic Limit and Plasticity Index of Soils*, American Association of State Highway and Transportation Officials, Washington, DC.*

AASHTO, T. 99-01, (2009). Standard Method of Test for Moisture-Density Relations of Soils Using a 2.5-kg (5.5-lb) Rammer and a 305-mm (12-in.) Drop*, American Association of State Highway and Transportation Officials, Washington, DC.*

ASTM, C. 215, (2002). Standard test method for fundamental transverse, longitudinal, and torsional resonant frequencies of concrete specimens*, American Society for Testing and Materials, Philadelphia, PA*.

ASTM, E2583, (2007). Standard Test Method for Measuring Deflections with a Light Weight Deflectometer (LWD). *Annual Book of Standards, ASTM International, West Conshohocken, PA*.

ASTM, E2835-11, (2011). Standard test method for measuring deflections using a portable impulse plate load test device.

Choo, L. P., & Yanful, E. K. (2000). Water flow through cover soils using modeling and experimental methods. *Journal of Geotechnical and Geoenvironmental Engineering*, *126*(4), 324-334.

Das, B. M. (2014). *Advanced soil mechanics*. CRC Press.

Faure, P., & Coussot, P. (2010). Drying of a model soil. *Physical Review E*, *82*(3), 036303.

Fredlund, D. G., & Xing, A. (1994). Equations for the soil-water characteristic curve. *Canadian geotechnical journal*, *31*(4), 521-532.

Gitirana, G., (2004). Weather-Related Geo-Hazard Assessment Model for Railway Embankment Stability, Doctoral dissertation, University of Saskatchewan, Saskatoon, SK, Canada.

Han, J., & Zhou, Z. (2013). Dynamics of soil water evaporation during soil drying: laboratory experiment and numerical analysis. *The Scientific World Journal*, *2013*.

Khire, M. V., Benson, C. H., & Bosscher, P. J. (1997). Water balance modeling of earthen final covers. *Journal of Geotechnical and Geoenvironmental Engineering*, *123*(8), 744-754.

Khosravifar, S. (2015). *Large-scale controlled-condition experiment to evaluate light weight deflectometers for modulus determination and compaction quality assurance of unbound pavement materials* (Doctoral dissertation, University of Maryland, College Park).

Lu, Y. (2015). Temperature Effect on Unsaturated Hydraulic Properties of Two Fine-Grained Soils and Its Influence on Moisture Movement Under an Airfield Test Facility. Arizona State University.

Machibroda, R., Wilson, G.W., and Barbour, S.L. 1993. A laboratory characterization of the properties of the Waite Amulet cover materials for evaporative flux modelling. University of Saskatchewan, Report prepared for the Noranda Technology Centre.

Pacheco, L., & Nazarian, S. (2011). Impact of moisture content and density on stiffness-based acceptance of geomaterials. *Transportation Research Record: Journal of the Transportation Research Board*, (2212), 1-13.

Wilson, G. W. (1990). Soil evaporative fluxes for geotechnical engineering problems, Doctoral dissertation, University of Saskatchewan, Saskatoon, SK, Canada.

Wilson, G. W., Fredlund, D. G., & Barbour, S. L. (1994). Coupled soil-atmosphere modelling for soil evaporation. *Canadian Geotechnical Journal*, *31*(2), 151-161.

Yanful, E. K., & Choo, L. P. (1997). Measurement of evaporative fluxes from candidate cover soils. *Canadian Geotechnical Journal*, *34*(3), 447-459.

Yanful, E. K., Mousavi, S. M., & Yang, M. (2002). Modeling and measurement of evaporation in moisture-retaining soil covers. *Advances in Environmental Research*, *7*(4), 783-801.

https://www.decagon.com/en/soils/volumetric-water-content-sensors/gs1/

https://www.soilvision.com/subdomains/svflux.com/index.shtml